Rhamm-/- mice are defective in skin wound repair due to aberrant ERK1,2 signaling in fibroblast migration.

Cornelia Tölg[1], Sara R. Hamilton[2], Kari-Anne[3], Paul Walton[3], James B. McCarthy[4], Mina J. Bissell[5], Eva A. Turley[3*]

[1]London Regional Cancer Program, Cancer Research Laboratories (London, Ontario, Canada);
[2]London Regional Cancer Program, Cancer Research Laboratories (London, Ontario, Canada) and Department of Biochemistry, University of Western Ontario (London, Ontario, Canada);
[3] Department of Anatomy and Cell Biology, University of Western Ontario (London, Ontario, Canada)
[4]Department of Laboratory Medicine and Pathology and University of Minnesota Comprehensive Cancer Center (Minneapolis, MN, USA);
[5]Life Sciences Division, Lawrence Berkeley National Laboratory (Berkeley, CA, USA).

*** To whom correspondence should be addressed**
London Regional Cancer Program
790 Commissioners Rd E, London, Ontario, Canada N6A4L6
Business Phone: 519-685-8600 ext 53677 FAX: 519-685-6816
Home Phone: 519-675-1883 Email: eva.turley@lhsc.on.ca

Condensed title: Repair of skin wounds is aberrant in Rhamm-/- mice

Key words: hyaluronan, Rhamm, CD44, ERK1, CD168, fibroplasia, wound repair

Number of characters (not including Materials and Methods): 49,815

Number of characters in Materials and Methods: 11,261

Number of words in Abstract: 161

ABSTRACT

Rhamm is a hyaluronan (HA) binding protein with limited expression in normal tissues and high expression in advanced cancers. Here we show that genetic deletion of Rhamm results in defective wound granulation tissue formation/resolution. Rhamm-/- (Rh-/-) fibroblasts migrate more slowly than Wt and fail to resurface >3mm scratch wounds or invade HA-supplemented ECM gels. This defect appears to result from impaired CD44/ERK signaling that results in reduced motility speed. In Rhamm-expressing fibroblasts, Rhamm, CD44 and ERK1,2 form complexes and both Rhamm and CD44 are necessary for maximal activation of these MAP kinases and maximal motility speed. Rhamm is required to promote cell surface display of CD44 and CD44/ERK1,2 co-localization since Rh-/- fibroblasts exhibit reduced surface CD44, reduced ERK/CD44 co-association and aberrant activation/subcellular targeting of ERK1,2. Signaling defects and impaired motility are rescued by either expression of mutant active MEK1 or restoration of cell surface Rhamm (CD168). These results identify Rhamm as an essential regulator of CD44/ERK1,2 motogenic-signaling required for wound repair.

INTRODUCTION

Rhamm is a HA-binding protein that is either not expressed or expressed at low levels in normal adult tissues but is highly expressed in aggressive human tumors (Adamia et al., 2005; Tammi et al., 2002; Toole, 2004). Analyses of animal models have confirmed instructive roles for Rhamm in tumorigenesis and in other disease processes such as arthritis. Roles for Rhamm in these diseases are consistent with its well-documented *in vitro* functions in migration and proliferation/apoptosis (Turley et al., 2002). Since migration and proliferation/apoptosis are essential functions for morphogenesis and tissue homeostasis, it is surprising that genetic deletion of Rhamm does not affect embryogenesis or adult homeostasis. Indeed, to date, a physiological function for Rhamm has remained elusive.

Rhamm was originally isolated from subconfluent migrating fibroblasts (Turley, 1982) and subsequently cloned from mesenchymal progenitor cells (Hardwick et al., 1992). Antibodies prepared against a shed form of Rhamm block HA-stimulated-fibroblast motility, suggesting that Rhamm is a cell surface protein that transduces motogenic signaling pathways *in culture* (Turley et al., 2002). Rhamm-bound HA is detected in cancer cell lines (Adamia et al., 2005) and shown to exist also in intracellular compartments/structures including the actin and microtubule cytoskeletons, nucleus and cytoplasm (Adamia et al., 2005). These results suggest that Rhamm has extracellular and intracellular functions. However, whether or not Rhamm acts as a cell surface receptor for HA became controversial partly because cloning of the human (Crainie et al., 1999; Hofmann et al., 1998; Wang et al., 1996) and mouse genes (Hofmann et al., 1998) revealed an absence of both a signal peptide required for export through the golgi/ER and membrane spanning domain(s) common to most cell surface receptors. In this and other characteristics, Rhamm resembles a group of intracellular proteins (e.g. epimorphin/syntaxin-2, autocrine motility factor/phosphoglucose isomerase) that also lack these signature characteristics of cell membrane receptors but which are nevertheless found at the cell surface and transmit signals across the cell membrane to regulate a number of cellular functions (Nickel, 2005; Radisky et al., 2003).

We have shown that Rhamm expression is high in aggressive fibromatoses (desmoid) tumors (Tolg et al., 2003). We further demonstrated that genetic deletion of Rhamm strongly reduced desmoid tumor initiation and invasion in a mutant APC and β-catenin-driven mouse model of this mesenchymal tumor. Fibroproliferative processes such as aggressive fibromatosis resemble proliferative/migratory stages of wound healing (Cheon et al., 2002). The expression

of Rhamm is modulated during wounding (Lovoorn et al., 1998) and by fibrogenic cytokines such as TGF-β (Samuel et al., 1993). Since factors that regulate fibroblast function play dual roles in wound repair and tumorigenesis (Bissell, 2001; Park et al., 2000), we have assessed in the current study whether Rhamm is involved in repair of excisional skin wounds using Rh-/- mice. The results show that Rhamm loss results in defects in early phases of skin repair, in particular in granulation tissue formation and resolution. This defect is associated with impaired migration/motility of fibroblasts and is due to aberrant kinetics of ERK1,2 activation/subcellular targeting.

RESULTS

Rhamm expression is required for granulation tissue formation and resolution in skin wounds.

Rhamm expression increases during repair of excisional wounds on human skin xenografts in immune compromised mice (Lovvorn et al., 1998) and following scratch wound of smooth muscle cell monolayers *in culture* (Savani et al., 1995). In the present study, Rhamm expression was followed during the first 7 days after excisional wounding of mouse skin. RT-PCR analysis of wounds showed that Rhamm expression was low in uninjured skin (Suppl. Fig. Ia). A marked increase in Rhamm mRNA was obvious one day after injury and expression was increased until d ay 3 when mRNA levels began to drop. By day 7 Rhamm mRNA levels were only slightly higher than those observed in uninjured skin. These results indicate that Rhamm is expressed during the early stages of excisional skin wound repair, which include wound contraction, re-epithelialization and granulation tissue formation. We therefore next assessed the consequences of Rhamm loss to the integrity of these early processes by photographing wound sites and by analyzing serial cross sections cut through wound centers.

Wt and Rh-/- wounds both contracted by day 1-3 after injury, but contraction of day 3 Rh-/- wounds was significantly reduced compared to Wt wounds (Suppl. Fig. Ib). Differences in wound contraction were not detected at later times when wound areas were measured from photographs (Suppl. Fig. Ib). By day 14, Wt and Rh-/- wound sites both appeared resolved at the macroscopic level ("unpublished data"). However, when the distance between wound edges was measured using tissue sections cut through wound centers, significant reductions in the contraction of Rh-/- wounds could be detected at days 1 and 3 but also at day 14 (Suppl. Fig. Ic). Since granulation tissue myofibroblasts contribute to wound contraction, since loss of Rhamm results in a significant decrease in the thickness of the dermis before injury (Suppl. Fig.IIa) and since resolution of Rh-/- dermis was delayed, as indicated by continued fibroplasia and reduced differentiation of dermal structures (day 21, Suppl. Fig. IIb), we next focused upon the consequences of Rhamm loss on granulation tissue formation/resolution.

A temporal spatial defect in the formation and resolution of granulation tissue was observed in Rh-/- vs. Wt wounds (Fig. 1A, B). Tenascin-positive granulation tissue was abundant in day 3 Wt wounds and began to decrease by day 7 (Fig. 1A). At day 14, wound granulation tissue was largely resolved in Wt mice (Fig. 1A, B). In contrast, the area of tenascin-positive granulation tissue in day 3 and 7 Rh-/- wounds was significantly smaller than in Wt wounds. Day 14 wounds of Rh-/- mice were

still strongly tenascin-positive, although the areas of these regions were highly variable between Rh-/- mice (Fig. 1A, B). Interestingly, the pattern of tenascin staining in day 14 Rh-/- wounds was abnormal as the staining was “patchy”, in contrast to day 14 Wt wounds (Fig. 1A). An additional difference in Rh-/- wounds was the transient appearance of a thick layer of subcutaneous adipocytes in day 1-3 Rh-/- wounds (Fig. 2A and “unpublished data”). These results indicate that a prominent effect of Rhamm deficiency during wound repair is a miscuing of signals required for the temporal regulation of granulation tissue formation and resolution.

Fibroplasia is a particularly prominent feature of granulation tissue in excisional skin wounds. The biological activities of fibroblasts and other mesenchymal cells, such as myofibroblasts, are key factors in the formation of early granulation tissue architecture (Reid et al., 2004). Robust fibroplasia, as quantified by the density/unit area of granulation tissue fibroblasts, was apparent in day 3 Wt wounds and was increased by day 7 (Fig. 2A). Myofibroblasts, detected by smooth muscle actin staining, were also abundant in Wt wounds by day 7 (Fig. 2B). Fibroplasia was observed in day3/7 Rh-/- granulation tissue but was blunted appreciably in comparison to Wt wounds (Fig. 2A) and there was a significant decrease in the number of myofibroblasts in day 7 Rh-/- wounds compared to Wt (Fig. 2B). Furthermore, Rh-/- granulation tissue was confirmed to contain abundant adipocytes, particularly at the wound edge, as indicated by the presence of vacuolated cells (Fig. 2A, arrows) which stained strongly with the lipophylic dye, BODIPY493/503 (Gocze and Freeman, 1994) ("unpublished data "). Rh-/- cells explanted from normal skin (day 0) and from day 7 wounds expressed less smooth muscle actin and accumulated more lipid than explanted Wt cells (Fig. 2C). Thus, deletion of Rhamm results in lower fibroblast density and aberrant differentiation in Rh-/- granulation tissue.

A number of factors can affect fibroplasia as granulation tissue forms. For example, a chronic inflammatory response at the wound site is required to initiate fibroplasia and functions to provide growth factors and cytokines that attract fibroblasts into the wound site. These factors regulate fibroblast migration, survival and proliferation (O'Leary et al., 2002). Rhamm regulates white cell trafficking *in vivo* and proliferation/ apoptosis *in culture* (Adamia et al., 2005; Turley et al., 2002). Surprisingly, *in vivo* analysis revealed a significantly *greater* percentage of polymorphonuclear cells (cell/field) in Rh-/- day 3 and day 7 granulation tissue (65 ± 6; 40 ± 12) compared to Wt (42 ± 8 and 8 ± 1, respectively) suggesting that Rhamm loss results in prolonged acute inflammation within excisional wounds. However, proliferation, as measured by the number of murine Ki-67-positive nuclei in granulation tissue, was not significantly different

from Wt, nor was the rate of apoptosis significantly different in Rh-/- vs. Wt wounds when measured by ApopTag staining ("unpublished data"). While these data do not rule out a role for fibroblast proliferation/apoptosis in the blunted fibroplasia observed in Rh-/- wounds *in vivo*, they suggest that these are not dominant factors.

Rhamm expression is required to sustain ERK1,2 activation during granulation tissue formation in vivo and in fibroblasts responding to growth factors in culture.

Fibroblast migration also contributes to fibroplasia and requires appropriate temporal regulation of signaling pathways such as ERK1,2, which provide cues for promoting and sustaining migration/invasion (Krueger et al., 2001). Furthermore, these MAP kinases have been implicated in mesenchymal differentiation into adipocytes, the most prominent being ERK1 (Bost et al., 2005). Since we have shown that Rhamm associates with ERK1 in fibroblasts and that this association is required for PDGF-BB stimulated ERK1,2 activation (Zhang et al., 1998), we hypothesized that the activity of these MAP kinases may be deficient in Rh-/- wound granulation tissue and contribute to aberrant fibroblast migration/differentiation (Hornberg et al., 2005). Wt granulation tissue fibroblasts exhibited strong staining for the active forms of these kinases, as assessed with anti-phospho-ERK1,2 antibodies, at day 3 after wounding (Fig. 3). At this time, levels of phospho-ERK1,2 were also similar for Rh-/- vs. Wt granulation tissue, when standardized against total ERK1,2 levels (Fig. 3, graph). Staining intensity for phospho-ERK1,2 in Wt granulation tissue fibroblasts increased 6-fold by day 7 and did not drop significantly until day 13, whereas staining intensity of phospho-ERK1,2 had prematurely decreased in Rh-/- granulation tissue by day 7 (Fig. 3). These changes in active ERK1,2 of Rh-/- vs. Wt granulation tissue fibroblasts were not due to decreases in total ERK1,2 protein levels since immunoblot analyses revealed that Rh-/- fibroblasts expressed similar amounts of ERK1,2 protein compared to Wt fibroblasts *in vivo* ("unpublished data"). These results indicate that ERK1,2 activity in Rh-/- granulation tissue fibroblasts is aberrant and may contribute to the miscuing of granulation tissue formation/resolution of Rh-/- excisional wounds.

To determine whether the aberrant ERK1,2 activity observed in Rh-/- granulation tissue fibroblasts *in vivo* is a cell autonomous or micro-environmental defect, we quantified the response of isolated Rh-/- vs. Rh^{FL}-rescued Rh-/- fibroblasts to serum (FCS) (Fig. 4). ELISA analysis of active (phospho)-ERK1,2 revealed that both Rh^{FL}-rescued and Rh-/- fibroblasts activated ERK1,2 in response to serum (Fig. 4A) and to PDGF ("unpublished data") but activity

was slightly less and declined more rapidly in Rh-/- fibroblasts (Fig. 4A). Western blots confirmed these results (Fig. 4B).

Confocal analysis showed that both Rh^{FL}-rescued and Rh-/- fibroblasts activate and target ERK1,2 to the cell nucleus (Fig. 4C). However, significantly less activated ERK1,2 accumulated in the cell nucleus in a 10-60 min exposure to serum than Rh^{FL}-rescued counterparts (Fig. 4C). Importantly, very little activated ERK1,2 accumulated at the membrane of Rh-/- cell processes while these MAP kinases were clearly activated and targeted to cellular processes in Rh^{FL}-rescued fibroblasts or in Wt fibroblasts (Fig. 4C and "unpublished data"). These results suggest that Rhamm is required both for sustaining ERK1,2 activity in different subcellular compartments and for the appropriate temporal regulation of trafficking active ERK1,2, both of which could affect motility and differentiation (Hornberg et al., 2005).

Rhamm expression is required for fibroblast migration and invasion in culture assays.

To assess whether or not the above ERK1,2 activation/targeting deficiencies in Rh-/- fibroblasts result in a migration defect, the motogenic behaviour of Rh-/- and Wt fibroblasts were compared using scratch wound and 3D collagen gel assays designed to mimic aspects of migration within the wound microenvironment (Reid et al., 2004). Significantly fewer Rh-/- than Wt fibroblasts migrated across 3mm scratch wounds *in culture* (Fig. 5A), as quantified both by the number of fibroblasts present in the wound gap and by time-lapse cinemicrography of fibroblasts migrating from the wound edge into the wound. A similar difference in migration was also exhibited when comparing Rh-/- to Rh^{FL}-rescued fibroblasts ("unpublished data"). Vector analysis of time-lapse wound images revealed that the motility speed of Rh-/- fibroblasts was less than Wt (Fig. 5A). These results indicate that loss of Rhamm expression results in an inherent migration defect related to a reduced ability of fibroblasts to orient and locomote rapidly towards haptotactic cues.

The invasive properties of Rh-/- vs. Wt fibroblasts were also compared using 3D collagen type I gels. Gels were constructed with central plugs composed of collagen type I, PDGF-BB and HA, surrounded by fibroblasts enmeshed in the surrounding collagen gel (Fig. 5B). Migration of primary Rh-/- dermal fibroblasts into the central collagen gel plug containing PDGF-BB and HA was reduced by almost 90% compared to that of litter-matched Wt fibroblasts (Fig. 5B) confirming that Rh-/- fibroblasts exhibited intrinsic and severe defects in haptotaxis and invasion *in vitro*.

Rhamm, CD44 and ERK1,2 form complexes and these HA receptors are required for activating ERK1,2

We have recently shown that Rhamm, CD44 and ERK1,2 form complexes required for motility of aggressive breast cancer cells (Fard et al. 2006). To begin to identify the motogenic mechanisms that are deficient in Rh-/- fibroblasts, we therefore first assessed the co-association of Rhamm/CD44/ERK1,2 in Rhamm-expressing fibroblasts and the dependence of these cells on Rhamm and CD44 for activating ERK1,2. The standard form of CD44 is expressed in equivilant amounts in Rhamm-expressing and Rh-/- fibroblasts (Fig. 6A). Pull-down assays using recombinant Rhamm-Sepharose demonstrated the ability of Rhamm, CD44 and ERK1,2 to co-associate (Fig. 6B). Confocal analysis showed co-localization of Rhamm and CD44 in ends of cell processes and a subset of CD44-positive perinuclear vesicles in $Rhamm^{FL}$-rescued fibroblasts (Fig. 6C). CD44 and active ERK1,2 also co-localized in cell processes and in a subset of CD44-positive perinuclear vesicles (Fig. 6B). Both CD44 and cell surface Rhamm are required for activation of ERK1,2 and trafficking to the cell nucleus in response to serum since anti-CD44 and anti-Rhamm antibodies significantly reduced the intensity of nuclear phospho-ERK1,2 (Fig. 7A).

Rhamm, CD44 and ERK1,2 are required for motogenic responses to serum and HA

The motility of Rh^{FL}-rescued fibroblasts responding to FCS stimulation required cell surface Rhamm, cell surface CD44 and active ERK1,2 since anti-Rhamm as well as anti-CD44 antibodies blocked motility as did the MEK1 inhibitors UO126 (Fig. 7B) and PD98059 (data not shown). Furthermore, in contrast to Rh^{FL}-rescued fibroblasts, Rh-/- fibroblast motility was not significantly affected by Rhamm or CD44 antibodies, or by MEK1 inhibitors (Fig. 7B, dotted line). Since signaling through CD44 and ERK1,2 have previously been shown to be required for motogenic responses to HA (Robertson et al., 2006), motility speed Rhamm-expressing vs. Rh-/- fibroblasts stimulated by HA was also assessed. To render non-transformed cells sensitive to HA, fibroblasts can be pre-treated with PMA, which is required to activate protein kinase C-dependent processes, permitting motogenic responses to HA (Hall et al., 2001). A mixture of high molecular weight HA and oligosaccharides significantly promoted random motility of Wt fibroblasts when PMA was present compared to PMA-treated cells alone (Fig. 7C). In contrast, the HA formulation did not enhance Rh-/- fibroblast random motility. HA-mediated motility of Rh^{FL}-rescued fibroblasts required cell surface Rhamm since anti-Rhamm antibodies blocked the increase in motility (Fig. 7C).

Rhamm promotes cell surface display of CD44 and co-distribution of CD44 and ERK1,2.

The inability of Rh-/- fibroblasts to increase random motility particularly in response to HA was puzzling since both genotypes produce equivalent amounts of total cellular standard CD44 protein as detected in Western blots (Fig. 6A). We therefore first assessed whether CD44 protein localization was altered in Rh-/- fibroblasts. Confocal microcopy of CD44 immunofluorescence suggest that loss of Rhamm resulted in fewer intracellular CD44-positive vesicles (Fig. 6A). Since aberrant trafficking of endocytosed surface proteins can result in altered display at the cell surface (Robertson et al., 2006), we next assessed whether or not Rhamm expression influenced the appearance of cell surface CD44. Cell surface display of CD44 was reduced by the loss of Rhamm, as shown by live cell immunofluoresence (Fig. 8A). Furthermore, both inhibition of MEK1 using either UO126 (Fig. 8A) or PD098059 ("unpublished data"), and cell surface Rhamm, using anti-Rhamm antibodies (Fig. 8A), reduced surface display of CD44. These reagents were not likely to cause degradation of CD44 protein since increased intracellular vesicles were observed with confocal analysis in treated fibroblasts ("unpublished data"). Rhamm expression, including cell surface Rhamm, also regulated the co-association of CD44 with ERK1,2 (Fig. 8B). ERK1,2 activity has previously been reported to associate with and be required for non-clathrin coated vesicle trafficking of cell surface proteins. Furthermore inhibition of ERK1,2 activity concommitently promoted accumulation of intracellular vesicles and reduced cell surface display of proteins such as HLA (Robertson et al., 2006). Our results are consistent with a similar role for ERK1,2 activity in trafficking CD44 to the cell surface and suggest a novel mechanism by which ERK1,2 may regulate cell motility. Since Rh-/- cells clearly exhibited an ERK1,2 activation defect, we next assessed whether or not restoration of ERK1,2 activity in the absence of Rhamm is sufficient to restore cell surface CD44 display and rescue motility.

Expression of mutant active Mek1 rescues the migration defect of Rhamm-/- fibroblasts.

Expression of mutant-active Mek1 restored the ability of Rh-/- fibroblasts to sustain activation of ERK1,2 in response to FCS (Fig. 9A, B) and this effect was not enhanced further by co-expression of Rh^{FL} (Fig. 9A). As well, activated Mek1 in Rh-/- fibroblasts restored migration in scratch wound assays ("unpublished data"), and significantly promoted motility speed in the absence of Rhamm expression in response to FCS (Fig. 9C). Expression of mutant-active Mek1 in Rh-/- fibroblasts also promoted cell surface display of CD44 (Fig. 9C). These results suggest that Rhamm and Mek1 act on the same CD44-regulated motogenic signaling pathway

since Mek1 can compensate for Rhamm in restoring motile behavior. Since Rhamm occurs within intracellular compartments as well as on the cell surface (Turley et al., 2002), we next assessed which Rhamm form is required and/or sufficient for restoring ERK1,2 activation, CD44 cell surface display and motility speed.

Cell surface Rhamm is sufficient to restore motility, CD44 surface display in Rh-/- fibroblasts and to partially restore ERK1,2 activity

The ability of anti-Rhamm antibodies to reduce Wt and Rhamm-rescued fibroblast motility, ERK1,2 activity, cell surface display of CD44 and the co-association of CD44 with ERK1,2 suggested that this form of Rhamm plays a key role in motogenic signaling. Furthermore, the co-association of Rhamm with CD44 provided a testable mechanism by which cell surface Rhamm, which does contain membrane spanning sequence, could affect activation of signaling cascades such as Ras-ERK1,2 (Toole, 2004; Turley et al., 2002). However, use of blocking antibodies does not permit assessement of the relative roles of cell surface vs. intracellular Rhamm and these studies did not exclude a role for intracellular Rhamm forms in the above motogenic processes. To assess the consequences of cell surface Rhamm, alone and in the absence of intracellular Rhamm proteins, recombinant Rhamm protein covalently linked to Sepharose beads were added to Rh-/- fibroblasts and motility speed was quantified using timelapse micrography. Rhamm-beads significantly stimulated motility speed but only of Rh-/- fibroblasts in contact with beads and not of those that lacked bead contact (Fig. 10A). Recombinant GST-beads had no effect on the motility speed of Rh-/- fibroblasts whether or not these beads contacted cells. Both anti-CD44 (Fig. 10A) and anti-Rhamm antibodies ("unpublished data") significantly blocked recombinant Rhamm-bead stimulated motility of Rh-/- fibroblasts and fibroblasts deficient in both Rhamm and CD44 did not increase their motility in response to these beads (Fig. 10A). CD44 surface display was also dramatically increased in Rh-/- fibroblasts contacting Rhamm-beads (Fig. 8A). These results indicate that cell surface Rhamm is sufficient for CD44 receptor display and promotion of motility speed: intracellular Rhamm is not required for these functions.

To begin to assess the mechanisms by which cell surface Rhamm promotes the above motogenic signaling pathway, we first determined whether or not Rhamm-bead stimulated motility requires ERK1,2. The Mek1 inhibitor UO126 reduced motility speed of Rh-/- fibroblasts contacting Rhamm-beads (Fig. 10A). Furthermore, recombinant Rhamm beads also significantly stimulated ERK1,2 activation and translocation to the cell nucleus in Rh-/-

fibroblasts (Fig. 10B). Activity was not as high as that of Rhamm-rescued fibroblasts suggesting a possible role for intracellular Rhamm forms in the degree of ERK1,2 activation (Toole, 2004; Turley et al., 2002). Most importantly, Rhamm-bead induced activation of ERK1,2 as well as motility was blocked by anti-CD44 antibodies (Fig. 10A,B) implicating cell surface Rhamm/CD44 interactions in jointly regulating ERK1,2 activity required for increasing cell surface display of CD44 and activating motogenic signaling pathways.

DISCUSSION

This study identifies Rhamm as a fibrogenic factor that is required for appropriate timing and spatial regulation of granulation tissue formation and resolution. A major consequence of Rhamm loss on granulation tissue formation/resolution is reduced/delayed fibroplasia associated with sparse fibroblast density, enhanced neutrophil accumulation and aberrant mesenchymal differentiation as indicated by reduced myofibroblast conversion and increased adipocyte accumulation within wound granulation tissue. Our studies also suggest that an underlying signaling defect associated with these repair deficiencies in Rh-/- wounds is de-regulated ERK1,2 activation that impacts upon signaling pathways promoting fibroblast migration and that affect mesenchymal cell differentiation. This conclusion is supported by the demonstration that Rh-/- fibroblasts retain their inability to appropriately activate ERK1,2 *in culture*, exhibit migration defects as measured by several locomotion assays, and that these defects are rescued by expression of mutant active Mek1, an ERK1,2 kinase activator. Our results further reveal an autocrine mechanism by which cell surface Rhamm promotes motility. This Rhamm protein form promotes ERK1,2 activation via a direct or indirect association with CD44, which in turn is required for maintaining cell surface display of CD44. ERK1,2 is acting downstream of cell surface Rhamm in this function since expression of mutant active Mek1 is sufficient to maintain cell surface CD44, activate ERK1,2 and restore motility in the absence of Rhamm expression. This motogenic mechanism is apparently required for both growth factor and HA-mediated motility. These findings identify for the first time a mechanism by which a non-integral Rhamm protein can activate intracellular signaling cascades and identify a novel mechanism by which ERK1,2 can promote motility.

ERK1 and 2 are closely related MAP kinase isoforms that can perform different physiological functions. For example, ERK2 is required for normal embryogenesis (Yao et al., 2003), whereas ERK1 plays more subtle and specific roles in adult physiology including adipogenesis (Bost et al., 2005). Both MAP kinases are activated by Mek1 or 2 and regulate signaling pathways that control cell motility, invasion and cytoskeleton remodeling during migration *in culture*. Our results show that these defects of Rh-/- fibroblasts result from an inability to sustain and maximally activate ERK1,2 following growth factor stimulation. These results are consistent with our previous evidence that cell surface Rhamm is required for PDGF-BB stimulated ERK1,2 activity in mesenchymal stem cells and for promoting migration by regulating signaling through upstream activators of ERK1,2 including HA, Src, Ras and FAK

(Hall et al., 1996; Hall et al., 1995; Turley et al., 2002). Others have also documented a role for cell surface Rhamm in activating signaling cascades that regulate motility and that directly or indirectly affect ERK1,2 activation (Aitken and Bagl, 2001; Goueffic et al., 2006; Lokeshwar and Selzer, 2000).

Although cell surface Rhamm can promote ERK1,2 activity to levels sufficient to sustain motility, it did not activate these MAP kinases to the levels achieved in the presence of both cell surface and intracellular Rhamm forms . Furthermore, although ERK1,2 activated in response to cell surface Rhamm translocated to the cell nucleus, these MAP kinases did not accumulate in the cell processes as was observed when intracellular Rhamm was also present. These results indirectly implicate intracellular Rhamm in the regulation of aspects of ERK1,2 activation/compartmentalization. These deficiencies did not affect the ability of cell surface Rhamm to promote motility speed but might affect other functions associated with ERK1,2 activity such as invasion and mitosis, neither of which were rescued by cell surface Rhamm alone ("unpublished data"). The consequences of ERK1,2 signaling to its functions in cell differentiation, migration and proliferation depends upon activation kinetics and subcellular compartmentalization (Colucci-D'Amato et al., 2003; Hendriks et al., 2005; Hornberg et al., 2005). These factors are determined by receptor dimerization, receptor internalization, "cross-talk" with other receptors, association of ERK1,2 with adaptor proteins, and activation of other kinases or phosphatases that modify ERK1,2 activity (Colucci-D'Amato et al., 2003; Hornberg et al., 2005). The possibility that cell surface Rhamm and intracellular Rhamm may differentially affect the activation levels and subcellular targeting of ERK1,2, which would have consequences to both transcription of motility- and invasion-related genes and phosphorylation of intracellular substrates that are involved in cell migration/invasion (Huang et al., 2004), merit further investigation.

ERK1,2 have previously been shown to regulate motility by both transcription and post-translational mechanisms. For example, initiation and early phases of migration during wound repair do not appear to require transcription (Providence and Higgins, 2004) but rather involve phosphorylation of predominantly cytoskeleton-associated (Helfman and Pawlak, 2005; Huang et al., 2004; Simoes and Fierro, 2005). Our results also identify a role for ERK1,2 activity in sustaining cell surface display of CD44, an integral membrane protein required for motility in response to growth factors and HA (Toole, 2004). ERK1,2 has previously been shown to promote recycling of clathrin-coated negative early endosomes back to the cell surface, a

pathway associated with recycling of B1 integrins and E-cadherin (Robertson et al., 2006). A similar ERK-regulated recycling event may be responsible for maintaining CD44 at the cell surface.

It is curious that motogenic responses to PDGF-BB or FCS are reduced but are not completely ablated in the absence of Rhamm while responses to HA are blocked. These results suggest a wider repertoire of mechanisms for regulating growth factor vs. HA mediated motility. The molecular mechanisms by which polysaccharides in general and HA in particular regulate physiological processes such cell migration during tissue repair are not yet well understood (Adamia et al., 2005; Toole, 2004). However, much like the closely related heparan sulfate, HA can impact signaling through associations with growth factor receptors involved in repair, including TGF-βR, and PDGFR, through receptors such as CD44 and Rhamm (Turley et al., 2002). One way in which HA has been shown to affect signaling through growth factors is by localizing growth factor receptors to specific cell surface membrane compartments. For example, HA and CD44 promote localization of fibrogenic receptors such as TGF-βR into lipid-rich rafts (Ito et al., 2004). This type of compartmentalization impacts the rate of internalization and intracellular trafficking of receptor/signaling complexes to endosomes and lysosomes for inactivation vs. recycling back to the cell surface. These parameters, in turn, have an effect on the kinetics of receptor activation including receptor-mediated activation of downstream effectors such as ERK1,2 (Hendriks et al., 2005) and likely speed of motility. These functions may affect a subset of growth factor receptors and have subtle but essential consequences to wound repair including promotion of cell motility speed, a factor in timely wound repair.

CD44 and Rhamm have overlapping functions in regulating migration events and Rhamm can compensate for loss of CD44 in aspects of splenocyte migration into arthritic joints (Nedvetzki et al., 2004). These and other studies (Goueffic et al., 2006; Turley et al., 1993) suggest that Rhamm can promote cell motility independently of CD44. Very likely in these instances cell surface Rhamm associates with other adhesion receptors involved in cell motility and partnering may depend upon expression and cell surface display levels of these receptors which will vary with disease, cell type and temporal stage of wound repair.

Rhamm belongs to a group of proteins that are predominantly intracellular but which can be exported to the cell surface via unconventional transport mechanisms that do not involve the export through the golgi/endoplasmic reticulum (Nickel, 2005). We show that cell surface Rhamm is displayed *in culture* after injury and our results have begun to clarify functions for cell

surface Rhamm vs. intracellular Rhamm protein forms. Although we did not define a role for intracellular Rhamm in cell motility, indirect evidence suggests that it plays a role in mitotic events *in culture* since cell surface Rhamm did not rescue the abnormal mitotic events observed during timelapse cinemicraphical analysis of Rh-/- fibroblasts. We, and others, have previously reported a role for Rhamm in regulating proliferation and in particular for progression through G2M of the cell cycle (Maxwell et al., 2005; Maxwell et al., 2003; Mohapatra et al., 1996; Tolg et al., 2003). Intracellular Rhamm proteins have been shown to associate with the interphase actin and microtubule cytoskeleton and to occur within the cell nucleus (Adamia et al., 2005; Turley et al., 2002). In particular, Rhamm protein associates with centrosomes and mitotic spindle microtubules (Evanko et al., 2004; Maxwell et al., 2003), and since microinjection of Rhamm antibody results in aberrant spindles and mitosis (Maxwell et al., 2003), it is likely that intracellular Rhamm forms play a role in mitosis. Nevertheless, our current data do not provide support for an essential role of Rhamm in mitotic spindle formation or cell cycle regulation during wound repair in dermal fibroblasts *in vivo,* as judged by the lack of detectable differences in proliferation or apoptotic indices within Rh-/- vs. litter-matched Wt wound sites. However, the slightly disorganized migration of Rhamm-/- fibroblasts from scratch wound assays on tissue culture plastic is consistent with a possible centrosomal defect that could contribute to aberrant migration (Watanabe et al., 2005) and merits further experimentation. A role for Rhamm in collagen contraction has also been controversial (Bagli et al., 1999; Travis et al., 2001). Unexpectedly, however, our studies have revealed a role for Rhamm in recruitment/differentiation of myofibroblasts and contraction of the wound bed. As is increasingly reported and recognized (Bissell et al., 2003), both of these results emphasize the importance of context and the microenvironment in regulating cell signaling. Thus, data obtained *in culture*, especially on two-dimensional (2D) substrata, need to be confirmed *in vivo* or at least in relevant microenvironments.

Collectively, our results are consistent with the conclusion that Rhamm is a fibrogenic factor expressed predominantly in cells that do not necessarily form parenchymal units. Cell surface Rhamm is required for promoting migration at least in part by regulating cell surface CD44 display via a CD44 dependent activation of ERK1,2 kinases. These *in culture* and physiological functions may provide a basis for understanding and further dissecting the importance of Rhamm hyperexpression in the invasion and metastasis of malignant tumors, as well as other disease processes.

MATERIALS AND METHODS

Reagents

Medical grade HA prepared from bacterial fermentation was the kind gift of Skye Pharma (London UK) and was free of detectable proteins, DNA or endotoxins (Filion and Phillips, 2001). The average molecular weight range and polydispersity of HA was 276.7kDa and 1.221kDa, respectively. HA oligosaccharides (MW_{avg} 10kDa) were a kind gift of Dr. F. Winnik (University of Montreal, QC) and were prepared by partial digestion with testicular hyaluronidase and purification by gel filtration. Human plasma fibronectin (BRL) , Ki67 (pAb, DAKO), α-smooth muscle actin (pAb, Santa Cruz), tenascin (pAb, Chemicon) and vimentin (pAb, Santa Cruz) antibodies and Oregon Green phalloidin (Molecular Probes) were used according to the manufacturer's instructions. Function blocking, affinity purified anti-Rhamm antibodies (Zymed) were confirmed to be specific by western blot and immunofluorescence assays of Rh-/- fibroblasts. Anti-CD44 antibodies (mAb, KM114 and IM7, Pharmingen) were confirmed to be specific using western and immunofluorescence analyses of CD44-/- dermal fibroblasts. Phospho-ERK1,2 antibodies (pAb, Cell Signaling Technology) were used for immunohistochemistry and immunofluorescence and phospho-ERK1,2 (mAb, Sigma) and pan-ERK1 antibodies (pAb, Santa Cruz,) were used for western blot analyses. Secondary antibodies were anti-rabbit Alexa 555 (Molecular Probes), Texas-Red or FITC labeled goat anti-mouse/goat anti-rabbit (Jackson laboratories), HRP-goat anti-mouse (Biorad), HRP-goat anti-rabbit (Pharmingen), HRP-rabbit anti-goat (Santa Cruz). All antibodies were used according to manufacturer's instructions. ABC staining system (Santa Cruz) was used for immunohistochemistry and ApoTag peroxidase *in situ* apoptosis detection kit (Chemicon) was used for quantification of apoptosis. FACE ERK1/2 ELISA kit (Active Motif) was used according to manufacturer's instructions to quantify ERK1/2 activation in response to FCS in Rh-/-, Rh^{FL}-, Mek1- and Mek1/Rh^{FL}-rescued cell lines. Mounting medium for immunofluorescence contained DAPI (Vectashield) while Cytoseal 60 (Richard-Allan Scientific) was used for mounting of tissue sections. The Mek1 inhibitors, PD98059 and U0126 (50μM and 10μM respectively, Biosciences), were used according to manufacturer's instructions. BODIPY 493/503 was purchased from Invitrogen and was used according to manufacturer's instructions.

Rh-/- mice; mouse embryonic fibroblasts and dermal fibroblasts

All animal experiments were performed in accordance with regulations of the animal use subcommittee at the University of Western Ontario, London, Ontario, Canada. The preparation

of Rh-/- mice and mouse embryonic fibroblasts (MEF), as well as genotyping of mice and fibroblasts, have been described (Tolg et al., 2003). CD44-/- mice have been described (Schmits et al , 1997). For the generation of Rh/CD44-/- double knock-out mice, heterozygous Rh+/- mice were crossed with homozygous CD44-/- mice resulting in Rh/CD44+/- mice. Mating between these Rh/CD44+/- heterozygous mice resulted in Rh/CD44-/- homozygous mice, which were identified by PCR as previously described (Schmits et al., 1997; Tolg et al., 2003). Dermal fibroblasts were isolated from explanted skin from newborn mice. For the isolation of cells from granulation tissue, wound punches were cut into small pieces and cultured with the dermal side facing down in complete cell culture medium (10% FCS, DMEM, antibiotic-antimycotic).

RT-PCR analysis of Rhamm and CD44 mRNA

Rhamm mRNA was amplified as previously described (Tolg et al., 2003) and PCR products were detected by Southern analysis using Rhamm exons 14-16 as a radioactive probe. CD44 mRNA was amplified as previously reported (Schmits et al., 1997). Amplification of *β-actin* mRNA was used as a loading control (Tolg et al., 2003).

Western blots

Western analyses of CD44, phospho-ERK1,2 and total ERK1,2 proteins were performed as described (Schmits et al., 1997; Tolg et al., 2003; Zhang et al., 1998). Densitometry was performed using Image Quant 5.1 software (Molecular Dynamics).

Recombinant protein production and in vitro pulldown assays

Recombinant Rhamm-GST fusion protein (murine Rhamm variant 4, 72kDa isoform) was expressed and purified as described previously (Mohapatra reference). Briefly, Rhamm-GST was expressed in bacteria and purified using Glutathione-sepharose beads (Amersham). Rhamm was released by thrombin digest (Amersham, as per manufacturer's guidelines), which cleaved Rhamm off of the GST tag. The beads were washed in PBS/1% Triton X-100. After several washes, a large amount of cleaved recombinant Rhamm protein remains associated with the glutathione sepharose beads and does not dissociate from the beads unless boiled in SDS. Control GST recombinant protein associated was also expressed and purified as described previously.

For the *in vitro* pull-down assays, recombinant Rhamm or recombinant GST beads were incubated with 500μg of whole Rh^{FL}-rescued cell lysate (prepared as described above) overnight at $4^{o}C$ on a nutator shaker. After overnight incubation beads were spun down and washed with cold lysis buffer. Proteins associated with beads were then boiled in SDS containing sample

buffer and were separated on a 10% SDS-PAGE, as described above). CD44s detection via western blot was done as described above.

Cell culture and transfection

Cell culture medium and culture conditions were described previously (Tolg et al., 2003; Zhang et al., 1998). PDGF-BB (25ng/ml), HA (500ng/ml-1mg/ml) or FCS (10%) were added to 24hrs serum-starved, 50% sub-confluent fibroblasts on fibronectin (25µg/ml)-coated dishes (Hall et al., 1996; Zhang et al., 1998). To obtain a response to HA, cells were pre-treated with 5nM PMA (Sigma) (Hall et al., 2001). For antibody blocking experiments cells were pre-incubated for 30 min with serum-free defined medium containing 10 µg/ml function blocking anti-Rhamm AB or control rabbit IgG prior to the addition of 10% FCS. Immortalized Rh-/- cells were transfected with Rh^{FL} murine Rhamm and/or mutant active Mek1 (kind gift of N. Ahn, U. Colorado, Boulder) in the presence of Lipofectamine Plus (Invitrogen) as described previously (Zhang et al., 1998). All transfectants were selected in G418 (1-5mg/ml for 2-3 weeks).

Excisional wounds and histology

Wt and Rh-/- mice (3-18 month old) were anaesthetized by Halothane inhalation. Two full thickness wounds were placed on denuded back skin using a 4mm metal punch. Mice were housed in individual cages for the experimental period. Wounds were harvested at varying times using a 8mm metal punch from similar locations on the backs of mice of the same gender and age. Harvested wounds were fixed overnight in 4% paraformaldehyde and paraffin embedded as described (Tolg et al., 2003). Numbered serial sections were cut perpendicular to the wound edge starting at the wound center. The first and last sections were stained with Masson's trichrome and non-stained sections were used for immunohistochemistry. To ensure that serial sections were cut starting at the wound center, wound samples were cut in half through the wound center prior to embedding

In total, five experimental series were performed. In each experiment, wounds were harvested at four different time points (1, 3, 7, and 14 days after wounding). For each time point, four age and gender matched mice were used (two Rh-/- and two Wt mice). In total, for each time point, ten Rh-/- and ten Wt mice were analyzed.

Immunohistochemistry of tissue sections and immunofluorescence of cultured cells

Tissue sections were stained for collagen (Masson's trichrome), α-smooth muscle actin, vimentin and tenascin following manufacturer's recommendations. Staining was quantified after counter-staining with Harris Hematoxylin (EM SCIENCE) and mounting in Cytoseal 60

(Tullberg-Reinert and Jundt, 1999). Immunofluorescence of phospho-ERK1,2 was done as previously published (Avizienyte et al., 2004). For detection of CD44 and Rhamm the protocol for phospho-ERK1,2 staining was followed with the exception that the primary ab was incubated over night at 4For the detection of droplets of neutral lipids, paraformaldehyde-fixed cells were stained with BODIPY 493/503 (25*u*g/ml) (Gocze and Freeman, 1994). Actin stress fibers were detected with Oregon-green phalloidin.

In vitro wound and invasion assays

Confluent cell monolayers on fibronectin coated dishes were serum starved overnight Scratch wounds (1 or 3 mm) were made using sized cell scrapers, then covered with medium containing 10% FCS or 25ng/ml PDGF-BB for 24-48hrs. Monolayers were fixed (3% paraformaldehyde), washed, stained with methylene blue (0.1% in methanol) then photographed using a Nikon inverted Eclipse TE 300 microscope. Images were analyzed for cell number per unit area of wound gap using Simple PCI (Compix). For 3D assays, collagen (Vitrogen100, Cohesion) or Matrigel (BD) gels were prepared according to manufacturers instructions. Plastic inserts were placed in the gel center. Fibroblasts were ($5x10^5$cells/ml) added to the outer gel ECM solution. After 24-48hrs, plastic inserts were removed and the cell free space was filled with collagen containing 25ng/ml PDGF-BB, 100μg/ml HA, and 25ng/ml fibronectin. Gels were fixed and analyzed 72hrs later for cell numbers/unit area.

Microinjections

Rh^{Fl}-rescued and Rh-/- fibroblasts were plated on fibronectin-coated glass coverslips in DMEM + 10% FCS. Approximately 2-4 hrs after plating, when cells had adhered, medium was replaced with defined DMEM containing transferrin and insulin. Cells were microinjected with function blocking anti-Rhamm AB or control rabbit IgG that had been concentrated to 3mg/ml in PBS using Microcon Centrifugal Filter Devices (Millipore). The microinjection was performed on a Leitz Labovert FS equipped with a micoinjector. Glass capillary needles (World Precision Instruments, Sarasota, FL) were prepared with a Kopf vertical pipette puller. Following Rhamm AB and control IgG miroinjection into the cell cytoplasm, cells were cultured for another 30 min in defined medium before they were stimulated with 10% FCS for either 10 or 30 min. Immunofluorescence for phospho-ERK1,2 and CD44 was performed and monitored with confocal microscopy as described above.

Time-lapse cinemicrography

For experiments assessing the motogenic effects of HA and PDGF-BB, cells were plated onto fibronectin-coated tissue culture flasks at 50% sub-confluence overnight then serum-starved for 24hrs. PDGF-BB or HA were added prior to filming as described (Hall et al., 2001; Zhang et al., 1998). For quantifying the effect of FCS, fibroblasts were plated at 50% sub-confluence overnight onto tissue culture dishes that had been pre-coated with serum proteins. FCS was added after a 24hr period of serum-starvation and cells were filmed as above.

Image acquisition, image enhancement, image analysis and statistical analysis s

Masson's trichrome and eosin/hematoxylin stained tissue sections as well as vimentin, tenascin and phospho-ERK1,2 stained tissue section images were taken with air objectives (4X, NA=0.16; 20X NA=0.7) using an Olympus AX70 Provis microscope equipped with a Cooke SensiCam color camera (CCD Imaging) and Image Pro Plus Version 4.5.1.2.9 software (Media Cybernetics, Inc.). For quantification of pERK1,2 staining, images were saved as tiff files and quantification of histology staining was done using Photoshop 6.0 (Adobe). The area of blue Hematoxylin staining, representing number of cells, was quantified by selecting and counting blue pixels (select, color range, blue, Image, Histogram). After deletion of the selected blue pixels, the area stained by the peroxidase substrate DAB was identified by selecting shadows (select, color range, shadows) and quantified by measuring the number of pixels (Image, Histogram). The area stained with tenascin was quantified using Simple PCI imaging software (Compix).

Images in Fig. 1A are composites of images taken with a 4x objective. The colors were enhanced using Photoshop 6.0 (Adobe, adjust, auto levels).

Scratch wound images were taken with air objectives (4x Nikon objective, air, NA=0.1, equipped with Hoffman modulation Contrast optics) using a Nikon Eclipse TE300 microscope equipped with a Hamamatsu digital camera (Hamamatsu) and Simple PCI imaging software (Compix). Images of the wounds were acquired using a Conica/Minolta Dimage Z3 digital camera equipped with 12x optical zoom. The wound area was quantified using Simple PCI imaging software (Compix). Immunofluorescent images of actin fluorescence (10x Nikon objective, air, NA=0.25) were also acquired using the Nikon Eclipse TE300 microscope and quantified using Photoshop 6.0 as above. Confocal images were taken using a 63X oil objective (Zeiss, NA=1.4) with a Zeiss 510 LSM Meta Confocal microscope using LSM 5 imaging

software (Zeiss). Fluorescence intensity of images was measured using LSM 5 imaging software (Zeiss).

Unless otherwise indicated in Figure Legends, comparisons between samples were assessed for statistical significance using a Student's "T" test, $p<0.05$ was considered significant a significant difference and is marked with an asterisk.

ACKNOWLEDGEMENTS

The technical assistance of Ms. Jenny Ma is gratefully acknowledged. This study was funded by a CIHR grant to E.T. (MOP-57694). Additional salary support was provided by The Breast Cancer Society of Canada (EAT), a CIHR fellowship and Breast Cancer Society of Canada fellowship (SRH, UST-63811), and a Postdoctoral Fellowship from the Translational Breast Cancer Research Traineeship Program (CT). JBM is supported in part by a grant from DA/DAMD 17-02-1-0102. MJB is supported by the USDOE (Office of the Biological and Environmental Research), by the USNCI and by an Innovator award from the USDOD Breast Cancer Program. ET and MJB are also the recipients of a BCRP-CDMRP grant (BC044087).

REFERENCES

Adamia, S., C.A. Maxwell, and L.M. Pilarski. 2005. Hyaluronan and hyaluronan synthases: potential therapeutic targets in cancer. *Curr Drug Targets Cardiovasc Haematol Disord*. 5:3-14.

Aitken, K., and D.J. Bagl. 2001. Stretch-induced bladder smooth muscle cell (SMC) proliferation is mediated by RHAMM-dependent extracellular-regulated kinase (erk) signaling. *Urology*. 57:109.

Avizienyte, E., V.J. Fincham, V.G. Brunton, and M.C. Frame. 2004. Src SH3/2 domain-mediated peripheral accumulation of Src and phospho-myosin is linked to deregulation of E-cadherin and the epithelial-mesenchymal transition. *Mol Biol Cell*. 15:2794-803.

Bagli, D.J., B.D. Joyner, S.R. Mahoney, and L. McCulloch. 1999. The hyaluronic acid receptor RHAMM is induced by stretch injury of rat bladder in vivo and influences smooth muscle cell contraction in vitro [corrected]. *J Urol*. 162:832-40.

Bissell, D.M. 2001. Chronic liver injury, TGF-beta, and cancer. *Exp Mol Med*. 33:179-90.

Bissell, M.J., A. Rizki, and I.S. Mian. 2003. Tissue architecture: the ultimate regulator of breast epithelial function. *Curr Opin Cell Biol*. 15:753-62.

Bost, F., M. Aouadi, L. Caron, and B. Binetruy. 2005. The role of MAPKs in adipocyte differentiation and obesity. *Biochimie*. 87:51-6.

Cheon, S.S., A.Y. Cheah, S. Turley, P. Nadesan, R. Poon, H. Clevers, and B.A. Alman. 2002. beta-Catenin stabilization dysregulates mesenchymal cell proliferation, motility, and invasiveness and causes aggressive fibromatosis and hyperplastic cutaneous wounds. *Proc Natl Acad Sci U S A*. 99:6973-8.

Colucci-D'Amato, L., C. Perrone-Capano, and U. di Porzio. 2003. Chronic activation of ERK and neurodegenerative diseases. *Bioessays*. 25:1085-95.

Crainie, M., A.R. Belch, M.J. Mant, and L.M. Pilarski. 1999. Overexpression of the receptor for hyaluronan-mediated motility (RHAMM) characterizes the malignant clone in multiple myeloma: identification of three distinct RHAMM variants. *Blood*. 93:1684-96.

Evanko, S.P., W.T. Parks, and T.N. Wight. 2004. Intracellular hyaluronan in arterial smooth muscle cells: association with microtubules, RHAMM, and the mitotic spindle. *J Histochem Cytochem*. 52:1525-35.

Filion, M.C., and N.C. Phillips. 2001. Pro-inflammatory activity of contaminating DNA in hyaluronic acid preparations. *J Pharm Pharmacol*. 53:555-61.

Gocze, P.M., and D.A. Freeman. 1994. Factors underlying the variability of lipid droplet fluorescence in MA-10 Leydig tumor cells. *Cytometry*. 17:151-8.

Goueffic, Y., C. Guilluy, P. Guerin, P. Patra, P. Pacaud, and G. Loirand. 2006. Hyaluronan induces vascular smooth muscle cell migration through RHAMM-mediated PI3K-dependent Rac activation. *Cardiovasc Res*.

Hall, C.L., L.A. Collis, A.J. Bo, L. Lange, A. McNicol, J.M. Gerrard, and E.A. Turley. 2001. Fibroblasts require protein kinase C activation to respond to hyaluronan with increased locomotion. *Matrix Biol*. 20:183-92.

Hall, C.L., L.A. Lange, D.A. Prober, S. Zhang, and E.A. Turley. 1996. pp60(c-src) is required for cell locomotion regulated by the hyaluronanreceptor RHAMM. *Oncogene*. 13:2213-24.

Hall, C.L., B. Yang, X. Yang, S. Zhang, M. Turley, S. Samuel, L.A. Lange, C. Wang, G.D. Curpen, R.C. Savani, and et al. 1995. Overexpression of the hyaluronan receptor RHAMM is transforming and is also required for H-ras transformation. *Cell*. 82:19-26.

Hardwick, C., K. Hoare, R. Owens, H.P. Hohn, M. Hook, D. Moore, V. Cripps, L. Austen, D.M. Nance, and E.A. Turley. 1992. Molecular cloning of a novel hyaluronan receptor that mediates tumor cell motility. *J Cell Biol*. 117:1343-50.

Helfman, D.M., and G. Pawlak. 2005. Myosin light chain kinase and acto-myosin contractility modulate activation of the ERK cascade downstream of oncogenic Ras. *J Cell Biochem*. 95:1069-80.

Hendriks, B.S., G. Orr, A. Wells, H.S. Wiley, and D.A. Lauffenburger. 2005. Parsing ERK activation reveals quantitatively equivalent contributions from epidermal growth factor receptor and HER2 in human mammary epithelial cells. *J Biol Chem*. 280:6157-69.

Hofmann, M., C. Fieber, V. Assmann, M. Gottlicher, J. Sleeman, R. Plug, N. Howells, O. von Stein, H. Ponta, and P. Herrlich. 1998. Identification of IHABP, a 95 kDa intracellular hyaluronate binding protein. *J Cell Sci*. 111 (Pt 12):1673-84.

Hornberg, J.J., B. Binder, F.J. Bruggeman, B. Schoeberl, R. Heinrich, and H.V. Westerhoff. 2005. Control of MAPK signalling: from complexity to what really matters. *Oncogene*.

Huang, C., K. Jacobson, and M.D. Schaller. 2004. MAP kinases and cell migration. *J Cell Sci*. 117:4619-28.

Ito, T., J.D. Williams, D.J. Fraser, and A.O. Phillips. 2004. Hyaluronan regulates transforming growth factor-beta1 receptor compartmentalization. *J Biol Chem*. 279:25326-32.

Krueger, J.S., V.G. Keshamouni, N. Atanaskova, and K.B. Reddy. 2001. Temporal and quantitative regulation of mitogen-activated protein kinase (MAPK) modulates cell motility and invasion. *Oncogene*. 20:4209-18.

Lokeshwar, V.B., and M.G. Selzer. 2000. Differences in hyaluronic acid-mediated functions and signaling in arterial, microvessel, and vein-derived human endothelial cells. *J Biol Chem*. 275:27641-9.

Lovvorn, H.N., 3rd, D.L. Cass, K.G. Sylvester, E.Y. Yang, T.M. Crombleholme, N.S. Adzick, and R.C. Savani. 1998. Hyaluronan receptor expression increases in fetal excisional skin wounds and correlates with fibroplasia. *J Pediatr Surg*. 33:1062-9; discussion 1069-70.

Maxwell, C.A., J.J. Keats, A.R. Belch, L.M. Pilarski, and T. Reiman. 2005. Receptor for hyaluronan-mediated motility correlates with centrosome abnormalities in multiple myeloma and maintains mitotic integrity. *Cancer Res*. 65:850-60.

Maxwell, C.A., J.J. Keats, M. Crainie, X. Sun, T. Yen, E. Shibuya, M. Hendzel, G. Chan, and L.M. Pilarski. 2003. RHAMM is a centrosomal protein that interacts with dynein and maintains spindle pole stability. *Mol Biol Cell*. 14:2262-76.

Mohapatra, S., X. Yang, J.A. Wright, E.A. Turley, and A.H. Greenberg. 1996. Soluble hyaluronan receptor RHAMM induces mitotic arrest by suppressing Cdc2 and cyclin B1 expression. *J Exp Med*. 183:1663-8.

Nedvetzki, S., E. Gonen, N. Assayag, R. Reich, R.O. Williams, R.L. Thurmond, J.F. Huang, B.A. Neudecker, F.S. Wang, E.A. Turley, and D. Naor. 2004. RHAMM, a receptor for hyaluronan-mediated motility, compensates for CD44 in inflamed CD44-knockout mice: A different interpretation of redundancy. *Proc Natl Acad Sci U S A*. 101:18081-6.

Nickel, W. 2005. Unconventional secretory routes: direct protein export across the plasma membrane of mammalian cells. *Traffic*. 6:607-14.

O'Leary, R., E.J. Wood, and P.J. Guillou. 2002. Pathological scarring: strategic interventions. *Eur J Surg*. 168:523-34.

Park, C.C., M.J. Bissell, and M.H. Barcellos-Hoff. 2000. The influence of the microenvironment on the malignant phenotype. *Mol Med Today*. 6:324-9.

Providence, K.M., and P.J. Higgins. 2004. PAI-1 expression is required for epithelial cell migration in two distinct phases of in vitro wound repair. *J Cell Physiol*. 200:297-308.

Radisky, D.C., Y. Hirai, and M.J. Bissell. 2003. Delivering the message: epimorphin and mammary epithelial morphogenesis. *Trends Cell Biol*. 13:426-34.

Reid, R.R., H.K. Said, J.E. Mogford, and T.A. Mustoe. 2004. The future of wound healing: pursuing surgical models in transgenic and knockout mice. *J Am Coll Surg*. 199:578-85.

Robertson, S.E., S.R. Setty, A. Sitaram, M.S. Marks, R.E. Lewis, and M.M. Chou. 2006. Extracellular signal-regulated kinase regulates clathrin-independent endosomal trafficking. *Mol Biol Cell*. 17:645-57.

Samuel, S.K., R.A. Hurta, M.A. Spearman, J.A. Wright, E.A. Turley, and A.H. Greenberg. 1993. TGF-beta 1 stimulation of cell locomotion utilizes the hyaluronan receptor RHAMM and hyaluronan. *J Cell Biol*. 123:749-58.

Savani, R.C., C. Wang, B. Yang, S. Zhang, M.G. Kinsella, T.N. Wight, R. Stern, D.M. Nance, and E.A. Turley. 1995. Migration of bovine aortic smooth muscle cells after wounding injury. The role of hyaluronan and RHAMM. *J Clin Invest*. 95:1158-68.

Schmits, R., J. Filmus, N. Gerwin, G. Senaldi, F. Kiefer, T. Kundig, A. Wakeham, A. Shahinian, C. Catzavelos, J. Rak, C. Furlonger, A. Zakarian, J.J. Simard, P.S. Ohashi, C.J. Paige, J.C. Gutierrez-Ramos, and T.W. Mak. 1997. CD44 regulates hematopoietic progenitor distribution, granuloma formation, and tumorigenicity. *Blood*. 90:2217-33.

Simoes, R.L., and I.M. Fierro. 2005. Involvement of the Rho-kinase/myosin light chain kinase pathway on human monocyte chemotaxis induced by ATL-1, an aspirin-triggered lipoxin A4 synthetic analog. *J Immunol*. 175:1843-50.

Tammi, M.I., A.J. Day, and E.A. Turley. 2002. Hyaluronan and homeostasis: a balancing act. *J Biol Chem*. 277:4581-4.

Tolg, C., R. Poon, R. Fodde, E.A. Turley, and B.A. Alman. 2003. Genetic deletion of receptor for hyaluronan-mediated motility (Rhamm) attenuates the formation of aggressive fibromatosis (desmoid tumor). *Oncogene*. 22:6873-82.

Toole, B.P. 2004. Hyaluronan: from extracellular glue to pericellular cue. *Nat Rev Cancer*. 4:528-39.

Travis, J.A., M.G. Hughes, J.M. Wong, W.D. Wagner, and R.L. Geary. 2001. Hyaluronan enhances contraction of collagen by smooth muscle cells and adventitial fibroblasts: Role of CD44 and implications for constrictive remodeling. *Circ Res*. 88:77-83.

Tullberg-Reinert, H., and G. Jundt. 1999. In situ measurement of collagen synthesis by human bone cells with a sirius red-based colorimetric microassay: effects of transforming growth factor beta2 and ascorbic acid 2-phosphate. *Histochem Cell Biol*. 112:271-6.

Turley, E.A. 1982. Purification of a hyaluronate-binding protein fraction that modifies cell social behavior. *Biochem Biophys Res Commun*. 108:1016-24.

Turley, E.A., L. Austen, D. Moore, and K. Hoare. 1993. Ras-transformed cells express both CD44 and RHAMM hyaluronan receptors: only RHAMM is essential for hyaluronan-promoted locomotion. *Exp Cell Res*. 207:277-82.

Turley, E.A., P.W. Noble, and L.Y. Bourguignon. 2002. Signaling properties of hyaluronan receptors. *J Biol Chem*. 277:4589-92.

Wang, C., J. Entwistle, G. Hou, Q. Li, and E.A. Turley. 1996. The characterization of a human RHAMM cDNA: conservation of the hyaluronan-binding domains. *Gene*. 174:299-306.

Watanabe, T., J. Noritake, and K. Kaibuchi. 2005. Regulation of microtubules in cell migration. *Trends Cell Biol*. 15:76-83.

Yao, Y., W. Li, J. Wu, U.A. Germann, M.S. Su, K. Kuida, and D.M. Boucher. 2003. Extracellular signal-regulated kinase 2 is necessary for mesoderm differentiation. *Proc Natl Acad Sci U S A*. 100:12759-64.

Zhang, S., M.C. Chang, D. Zylka, S. Turley, R. Harrison, and E.A. Turley. 1998. The hyaluronan receptor RHAMM regulates extracellular-regulated kinase. *J Biol Chem*. 273:11342-8.

ABBREVIATIONS

bFGF-2	Basic fibroblast growth factor-2
2D	2-dimensional culture
3D	3-dimensional culture
ECM	Extracellular matrix
ERK1,2	Extracellular regulated kinases 1,2
FAK	Focal adhesion kinase
HA	Hyaluronic Acid / Hyaluronan
Matrigel	Basement membrane matrix
MEFs	Mouse embryonic fibroblasts
Mek1	Mitogen activated kinase kinase 1
MMPs	Matrix metalloproteinases
MW	Molecular weight
Mw_{avg}	Average molecular weight
PDGF-BB	Platelet derived growth factor-BB
PDGFR	Platelet derived growth factor receptor
PMNs	Polymorphonuclear cells
Rhamm	Receptor for Hyaluronic Acid Mediated Motility
Rh^{FL}	Full-length Rhamm
Rh-/-	Rhamm -/-
TE	Tris-EDTA
TGF-β	Transforming growth factor-β
TGF-βR	Transforming growth factor-β receptor
Wt	Wild-type

FIGURE LEGENDS

Figure 1: Loss of Rhamm Delays and Alters the Pattern of Granulation Tissue Formation in Skin Wounds. *A. Tenascin Protein Expression in Wound Sections:* Wound granulation tissue is abundant in day 7 Wt wounds as indicated by positive staining for tenascin. Granulation tissue has largely resolved in Wt wounds by day 14 as indicated by restricted tenascin staining. The area of tenascin-positive Rh-/- granulation tissue is less in days 3 and 7 than Wt and has become aberrantly "patchy" by day 14, indicating delayed and abnormal patterning of granulation tissue resolution. Paraffin processed tissue sections were prepared perpendicular to the wound surface and cut at the wound center then stained for tenascin as a marker for granulation tissue. *B. Areas of Tenascin-Positive Granulation Tissue:* The area of Wt granulation tissue is significantly greater than Rh-/- at both day 3 and 7 after wounding ($p<0.01$ for both time points). High standard errors of tenascin-positive areas of Rh-/- granulation tissue reflect aberrant resolution patterns. Values represent the Mean and S.E.M. N= 4 tissue sections from 8 male mice for each genotype.

Figure 2: Loss of Rhamm Reduces Fibroblast Density and Increases Granulation Tissue Cell Heterogeneity. *A. Fibroblast Density in Granulation Tissue:* The density of fibroblasts is significantly reduced in Rh-/- granulation tissue at both day 3 ($p<0.0001$) and 7 ($p<0.001$) after wounding. Arrows indicate the presence of vacuolated cells, which are adipocytes. Fibroblast density is heterogeneous in Rh-/- granulation tissue (e.g. dotted circle is sparse; filled line circle is dense) but fibroblast density shown in graph was averaged per microscope field. Paraffin processed tissue sections were stained for vimentin. Values in graphs represent the Mean and S.E.M., N=4 sections from 8 animals for each genotype. *B. Smooth Muscle Actin-Positive Fibroblasts in Wounds:* The number of wound myofibroblasts is significantly reduced in day 7 Rh-/- wounds compared to Wt granulation tissue ($p<0.0001$). Paraffin processed tissue sections were stained for α-smooth muscle actin as described in Methods. Values in graphs represent the Mean and S.E.M., N=4 sections from 8 animals for each genotype. *C. Smooth Muscle Actin- and Lipid-Positive Fibroblasts (Adipocytes) in Granulation Tissue Explants in Culture*: The numbers of smooth muscle actin-positive fibroblasts are significantly reduced and the numbers of lipid-containing cells are significantly increased in Rh-/- granulation wound tissue when compared to Wt ($p<0.0001$). Cell outgrowths were stained with anti α-smooth muscle actin and

BODIPY493/503 as described in Methods. In confocal images, red staining is smooth muscle actin and green staining is BODIPY493/503 taken up into lipid droplets within cells. Laser settings were kept constant for Wt day 0 and Rh-/- day 0 images and for Wt day 7, Rh-/- day 7, IgG day 0 and acetone extracted day 0 images.

Figure 3: Loss of Rhamm Alters ERK1,2 Activation in Granulation Tissue Fibroblasts. Both Wt and Rh-/- granulation tissue fibroblasts are positive for activated (phospho)-ERK1,2 at day 3 after wounding. Staining for activated ERK1,2 significantly increases in Wt granulation tissue by day 7 ($p<0.001$), then drops by day 14. In contrast, staining drops to near background in day 7 Rh-/- wound granulation tissue ($p<0.00001$), and remains significantly lower than Wt at day 14 ($p<0.01$). Paraffin sections were stained with anti-phospho-ERK1,2 antibodies. Staining was quantified using image analysis and averaged per unit area of granulation tissue as described in Methods. Values represent the Mean and S.E.M., N=15 images of 3 tissue sections for each genotype (5 mice each).

Figure 4: Loss of Rhamm Reduces Serum Activation of ERK1,2 in Fibroblasts *in culture*. *A. ELISA Analysis of Total Cellular Phospho-ERK1,2:* Rh^{FL}-rescued fibroblasts sustain significantly higher levels of ERK1,2 activity at 30-60 min post serum stimulation than Rh-/- fibroblasts. Phospho-ERK1,2 in serum starved Rh^{FL}-rescued and Rh-/- fibroblasts exposed to serum were quantified as described in Methods. Values at 0 min were subtracted from values at 30 and 60 min. Values represent the Mean and S.E.M., N=3 samples. *B. Western Blot Analysis of Phospsho-ERK1:* Rh^{FL}-rescued fibroblasts sustain ERK1,2 activity between 10-50 min post serum stimulation while activity drops in Rh-/- fibroblast at 10 min. Anti-phospho-ERK1,2 antibodies were used to detect active ERK1,2 in western blots. *C. Confocal Micrographs and Image Analysis of Phospho-ERK1,2*: Micrographs and image analysis of Rh^{FL}-rescued and Rh-/- fibroblasts stained with anti-phospho-ERK1,2 antibodies confirm the significantly rapid drop in activated ERK1,2 observed in Rh-/- compared to Rh^{FL}-rescued fibroblasts, and show that targeting of phospho-ERK1,2 (red fluorescence) to the nucleus (blue fluorescence) is also significantly reduced in Rh-/- fibroblasts. Micrographs are taken from one of 4 similar experiments.

Figure 5: Loss of Rhamm Reduces Migration and Invasion of Wt and Rh-/- Primary Fibroblasts *A. Migration into Scratch Wounds in Response to FCS:* Significantly more Wt fibroblasts migrate into 3mm wound gaps than Rh-/- fibroblasts ($p<0.0001$). Values represent the Mean and S.E.M., N=6 randomly chosen wound areas. Time-lapse analysis of wound edges shows that Wt fibroblasts migrate at a higher speed and for longer distances than Rh-/- fibroblasts over a 24 hr period ($p<0.0001$). Values represent the Mean and S.E.M., N=3 experiments. *B. Invasion into Collagen Gels in Response to PDGF*: Diagram shows the construction of a collagen gel invasion assay where HA and PDGF-BB are present only in the central plug. A significantly greater number of Wt dermal fibroblasts migrate into central plugs than Rh-/- dermal fibroblasts ($p<0.00001$). Values represent the Mean and S.E.M., N=4 experiments.

Figure 6: CD44 Protein Co-Associates with Rhamm and Active ERK1,2 in Fibroblasts *A. CD44 Protein Expression:* Rh-/- fibroblasts express similar levels of CD44 proteins as Wt, as assessed by western blot analysis. β-actin was used as a protein loading control. *B. CD44 Protein Distribution:* Confocal analysis shows that CD44 (green fluorescence) is distributed in a similar pattern in both Rh^{FL}-rescued and Rh-/- fibroblasts but unlike Rh-/- fibroblasts, CD44 occurs predominantly within vesicles that co-associate with active ERK1,2 (red fluorescence) in Rh-/- ^{Fl}-rescued fibroblasts. Yellow fluorescence represents CD44 and phospho-ERK1,2 co-localization. IgG was used as a negative control for anti CD44 and anti phospho-ERK1,2. *C. Rhamm, CD44 and ERK1,2 Form Complexes:* Recombinant Rhamm coupled to sepharose beads (Rh-GST-Beads) pulls down both CD44 standard form (CD44s), a possible CD44 variant form and ERK1,2. GST coupled to beads (GST Beads) is used as a negative control for both assays. CD44s and ERK1,2 were detected by western analysis. Confocal analysis confirms that Rhamm (red fluorescence) and CD44 (green fluorescence) co-localize (indicated by white enhancement) in Rh-/- ^{Fl}-rescued fibroblasts in cell processes of fibroblasts that were not permealized with detergent and in vesicles of detergent permealized fibroblasts.

Figure 7: Cell Surface Rhamm (CD168) and CD44 are Required for ERK1,2 Activity and for Motility in Response to FCS and HA. *A. Role of CD168 (Rh) and CD44 in Nuclear ERK1,2 Activation.* $Rhamm^{FL}$-rescued fibroblasts were serum starved then stimulated with FCS in the presence of non-immune IgG, anti-Rhamm or anti-CD44 antibodies. Nuclear Phospho-

ERK1,2 staining was detected with confocal microscopy and quantified with image analysis. Both anti-Rhamm and anti-CD44 significantly reduced the levels of phosph-ERK1,2 in the cell nucleus in response to serum. Values represent one of four experiments and are the Mean and Standard Error of N=25 cells from a single experiment. *B. Rhamm-Rescued Cell Motility in Response to FCS:* Expression of $Rhamm^{FL}$ cDNA rescues random motility of Rh-/- fibroblasts. Motility speed of Rh-/- fibroblasts, which did not vary with the indicated treatment is represented by the dotted line. Rescue of motility by $Rhamm^{FL}$ requires surface CD44 expression and ERK1,2 activity since anti-CD44 and the Mek1 inhibitor, UO126, significantly reduce migration. The ability of anti Rhamm ab to block both Rh^{FL} confirms the specificity of this $Rhamm^{FL}$ effect. The values represent the Mean and S.E.M., N=30 cells and are the results of 1 of 6 similar experiments. *C. $Rhamm^{FL}$-rescued Motility in Response to HA:* In contrast to Wt, Rh-/- fibroblasts do not increase random motility in response to HA. Further, Rhamm antibodies reduce motility of Wt but not Rh-/- fibroblasts in the presence of HA. Fibroblasts were first exposed to PMA to generate responsiveness to HA. The values represent the Mean and S.E.M., N=30 cells and are the results of 1 of 4 similar experiments.

Figure 8: CD44 Cell Surface Display is ERK- and Cell Surface Rhamm-Dependent and Rhamm Promotes CD44/Phospho-ERK1,2 Co-Localization.

A. Effect of Rhamm and ERK1,2 Activity on Cell Surface CD44 Expression: Loss of Rhamm reduces surface display of CD44 compared to Rh^{Fl} rescued fibroblast. The Mek1 inhibitor UO126 and anti-Rhamm antibody also block CD44 cell surface display in Rh^{Fl} rescued fibroblasts. Recombinant Rhamm beads rescue CD44 cell surface expression on fibroblasts that touch or are close to the beads (arrows) indicating cell surface Rhamm is required for this Rhamm-dependent effect. *B. Effect of Rhamm on CD44 and Active ERK1,2 Co-localization:* Image analyses of Confocal micrographs (e.g. Figure 6B) of serum starved fibroblasts subsequently exposed to serum show Rhamm expression significantly promotes co-localization of CD44 and active ERK1,2 as quantified by pixel density of yellow fluorescence. Rhamm antibodies reduce this co-association in RhFL-rescued fibroblasts implicating cell surface Rhamm in this effect. Values represent one of 4 similar experiments and are the Mean and Standard Error of N=25 cells.

Figure 9: Mutant Active Mek1 Rescues Aberrant ERK1,2 Activity, Motility and CD44 Cell Surface Display in Rhamm-/- Fibroblasts. *A. ELISA Analysis of ERK1,2 Activity:* Expression of mutant active Mek1 in Rh-/- fibroblasts restores ERK1,2 activation ($p < 0.05$ for 30 and 60 min) in response to serum stimulation and activity is not further increased by co-expression of Rh^{FL} and mutant active Mek1. Phospho-ERK1,2 in serum starved Rh-/-, Mek1-rescued and Mek1/Rh^{FL}-rescued fibroblasts exposed to serum was quantified as described in Methods. Values at 0 min were subtracted from values at 30 and 60 min. Values represent the Mean and S.E.M., N=3 samples. *B. Western Blot Analysis of ERK1 Activity:* Western blot analyses confirms that expression of mutant active Mek1 rescues the ability of Rh-/- fibroblasts to activate ERK1. *C. Motility and Cell Surface CD44 Display in Rh-/- Fibroblasts Expressing Mutant Active Mek1:* Expression of mutant active Mek1 in Rh-/- fibroblasts significantly increases random motility speed of Rh-/- fibroblasts. Anti-CD44 signficantly significantly blocks migration of these Mek1-rescued Rh-/- fibroblasts. Values represent one of 3 similar experiments and are the Mean and S.E.M. of N=30 cells. Expression of Mek1 also restores cell surface display of CD44 to levels comparable to Rh^{FL}-rescued fibroblasts, as assessed by live cell immunofluorescence. The specificity of the anti-CD44 antibody is confirmed by lack of fluorescence in murine Rh-/- fibroblasts that also do not express CD44 (Rh-/- Cd44-/-).

Figure 10: Cell Surface Rhamm Rescues Motility Defect of Rh-/- Fibroblasts. *A. Cell Motility in Response to Recombinant Rhamm Beads:* Random motility of Rh-/- fibroblasts increases significantly when cells contact recombinant Rhamm beads whereas treatment with control GST-beads has no effect. Graphs show Mean and S.E.M. of 30 cells. Rhamm-bead-stimulated motility is similar to that of Rh^{FL}-rescued fibroblasts and also requires ERK1,2 activity and CD44 expression. *B. ERK1,2 Activation in Response to Recombinant Rhamm Beads:* ERK1,2 activation (red fluorescence) by Rh-/- fibroblasts in response to 10% FCS is significantly increased in cells exposed to recombinant Rhamm beads, compared to treatment with control GST-beads. Green fluorescence is CD44 staining. Image analysis was used to measure active ERK1,2 fluorescence in the cell nucleus. Values represent 1 of 3 similar experiments are are the Mean and Standard Error of N=25 cells.

Supplemental Figure I. Rhamm Expression is Regulated During Early Phases of Wound Repair and Loss of Rhamm Reduces Wound Contraction. *a. Rhamm Expression in*

Excisional Wounds: Rhamm mRNA expression is transiently up-regulated following excisional skin injury. Rhamm mRNA was amplified by RT-PCR and PCR products were visualized by Southern analysis using a Rhamm-specific probe. The band (arrow) represents the full-length Rhamm PCR product. RT-PCR of β-actin mRNA was used as a loading control. *b. Macroscopic Quantification of Wound Contraction:* Analyses of excisional areas from photographs of wounds show that Wt wounds contract more rapidly than Rh-/- wounds with a significant difference observed at day 3 after wounding ($p<0.05$). The circled area denotes forming granulation tissue, which is reduced in Rh-/- vs. Wt wounds. *c. Microscopic Quantification of Wound Contraction.* Analyses of tissue sections of wounds reveal a significant reduction in contraction at day 1 ($p<0.0001$), day 3 ($p<0.05$) and day 13 ($p<0.001$) in Rh-/- vs. Wt wounds. Wound contraction was measured as the distance between the edges of each wound site using tissue sections cut at the center of the excisional wound. Values represent the Mean and S.E.M. of 3 sections from 3 wounds of each genotype.

Supplemental Figure II. Loss of Rhamm Expression Results in Aberrant Dermal Structure and Thickness in Both Uninjured and Repaired Skin. *a. Dermis of Uninjured Skin:* The dermis of uninjured Wt skin (day 0) is significantly thicker than uninjured Rh-/- skin ($p<0.0001$). Sections were stained with Masson's Trichrome. *b. Dermis of Resolved Wounds:* The dermis at both the center and edges of Wt wounds at day 21 are resolved in that histology is similar to uninjured skin. Wt dermis is significantly thinner than Rh-/- wounds ($p< 0.0001$ and $p<0.01$). Rh-/- wounds have not fully resolved and wound site exhibits reduced dermal differentiation compared to Wt wounds (e.g. hair follicles have not formed shafts, subcutaneous lipid layer is not formed and muscle layer is not continuous at the underside of wounds). Paraffin-processed tissue sections were stained with Mason's trichrome to visualize dermal collagen (a, green stain) or hematoxylin/eosin to visualize cells (b). The thickness of the dermal layer was measured as the distance between the keratinocyte layer and the subcutaneous fat layer. Solid arrowheads mark the still discernable wound site in Rh-/- skin. Solid arrows mark undifferentiated hair follicles and open arrow heads indicate ongoing fibroplasia and incomplete muscle formation observed at the underside of Rh-/- wounds. Values represent the Mean and S.E.M. of 5 areas from 3 separate tissue sections for each experimental condition.

Figure 1. (Tolg et al.) Loss of Rhamm Delays and Alters the Pattern of Granulation Tissue Formation in Skin Wounds

A. Tenascin Protein Expression in Wound Sections

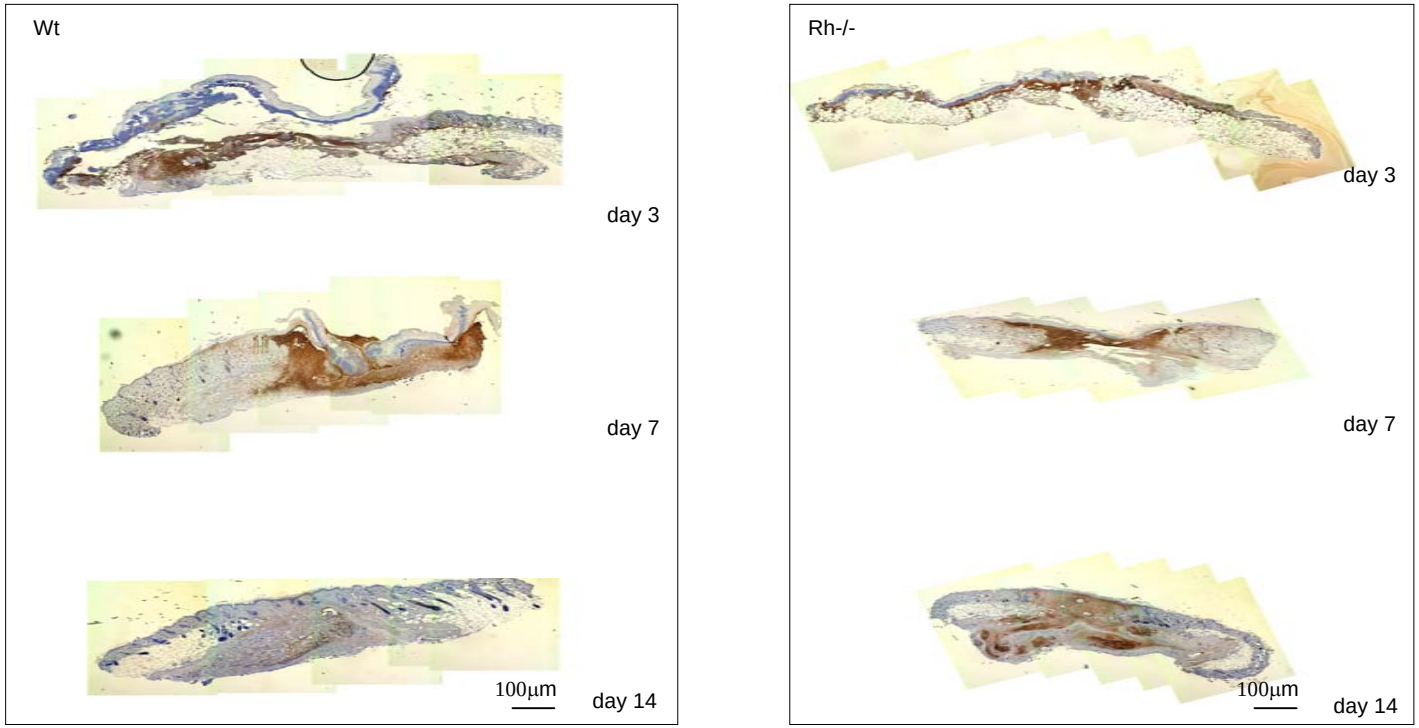

B. Areas of Tenascin-Positive Granulation Tissue

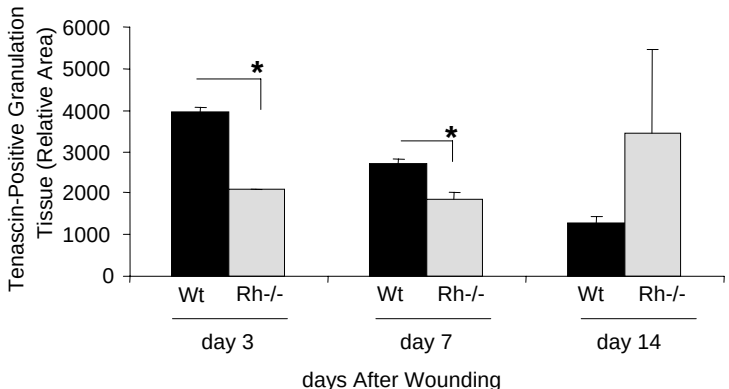

Figure 2. (Tolg et al.) Loss of Rhamm Reduces Fibroblast Density and Increases Granulation Tissue Cell Heterogeneity

A. Fibroblast Density in Granulation Tissue

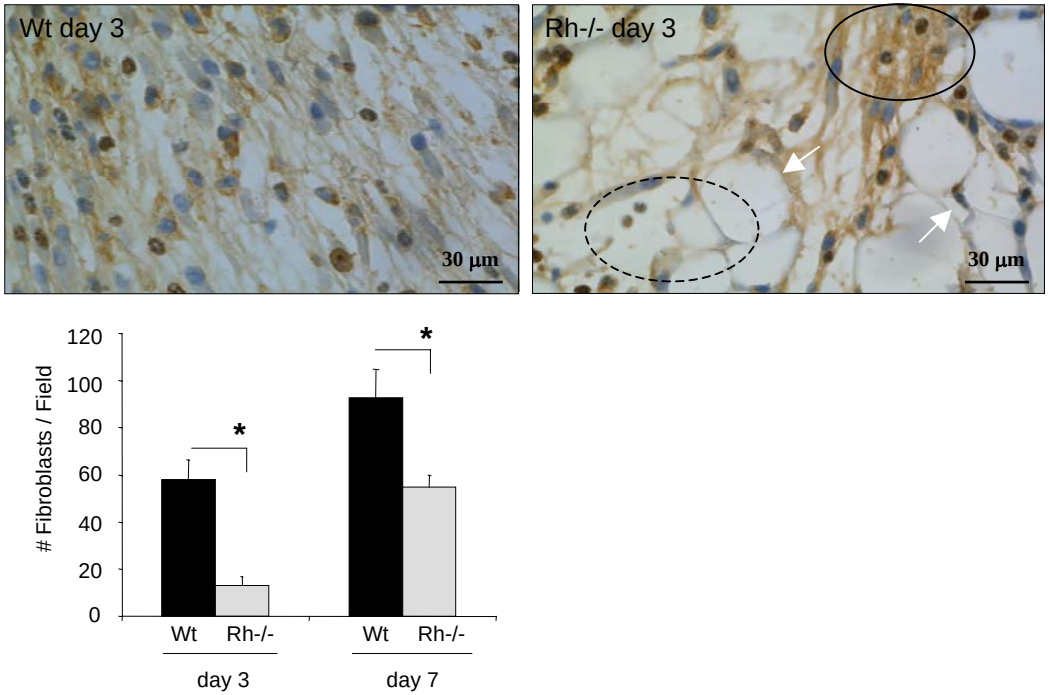

B. Smooth Muscle Actin-Positive Fibroblasts in Wounds

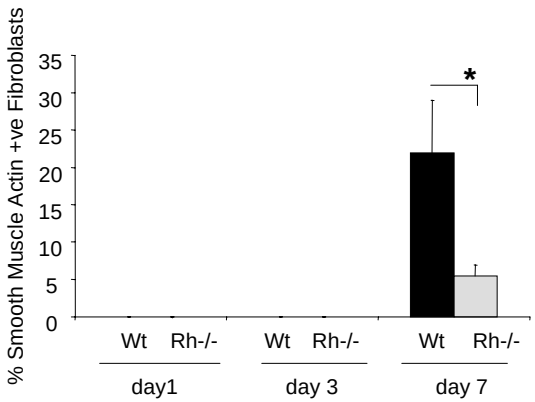

C. Smooth Muscle Actin and Lipid-Positive Fibroblasts (Adipocytes) in Granulation Tissue Explants *in Culture*.

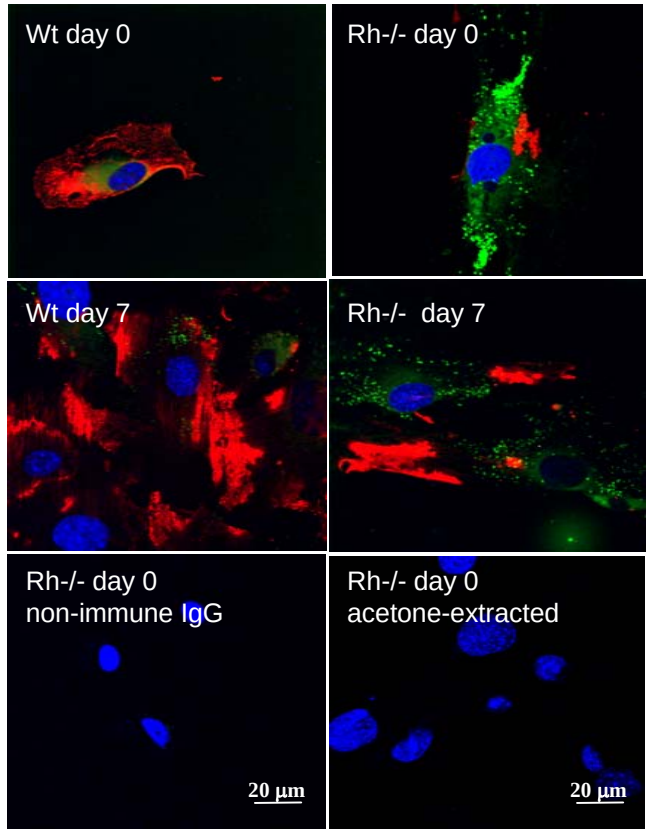

Figure 3. (Tolg et al.) Loss of Rhamm Alters ERK1,2 Activation in Granulation Tissue Fibroblasts

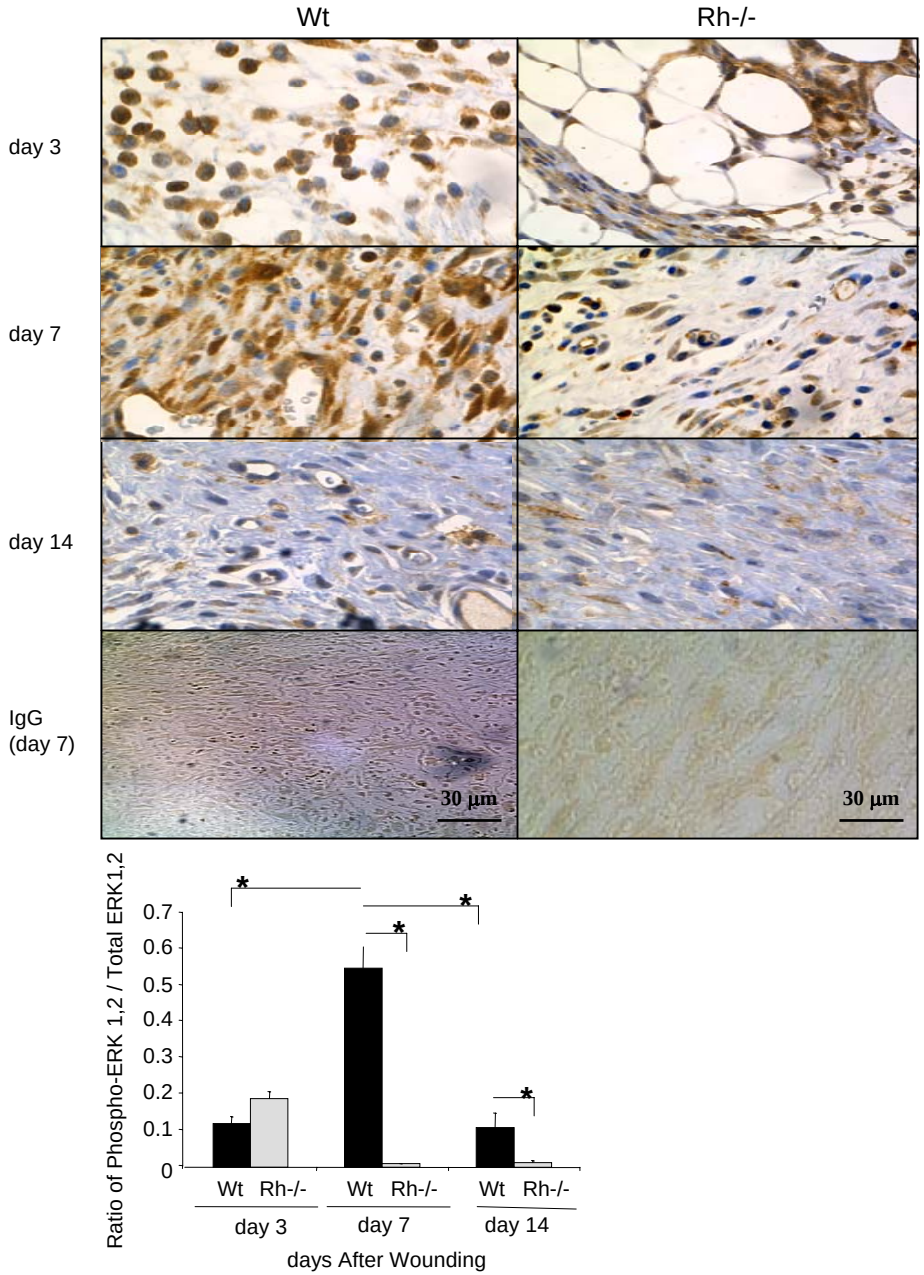

Figure 4. (Tolg et al.) Loss of Rhamm Reduces Serum Activation of ERK1,2 in Fibroblasts *in culture*

A. ELISA Analysis of Total Cellular Phospho-ERK1,2

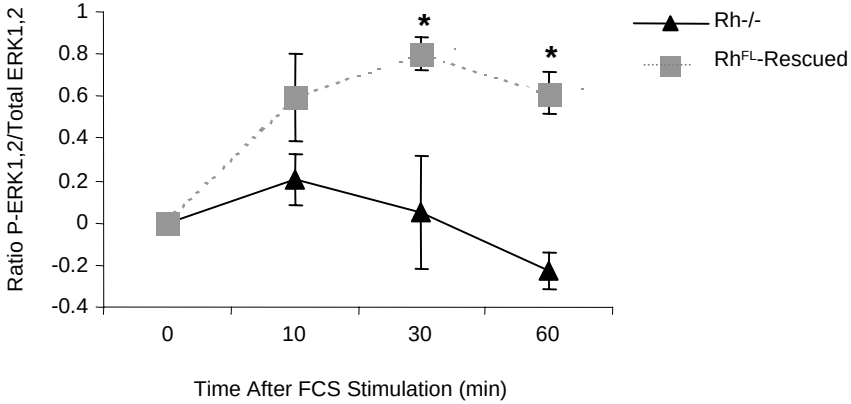

B. Western Blot Analysis of Phospho-ERK1

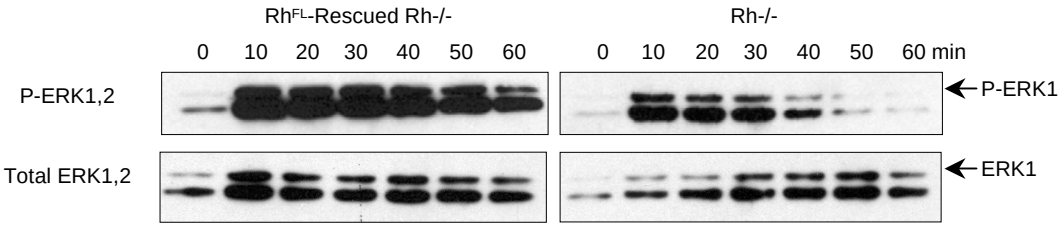

C. Confocal Micrographs and image analysis of Phospho ERK1,2

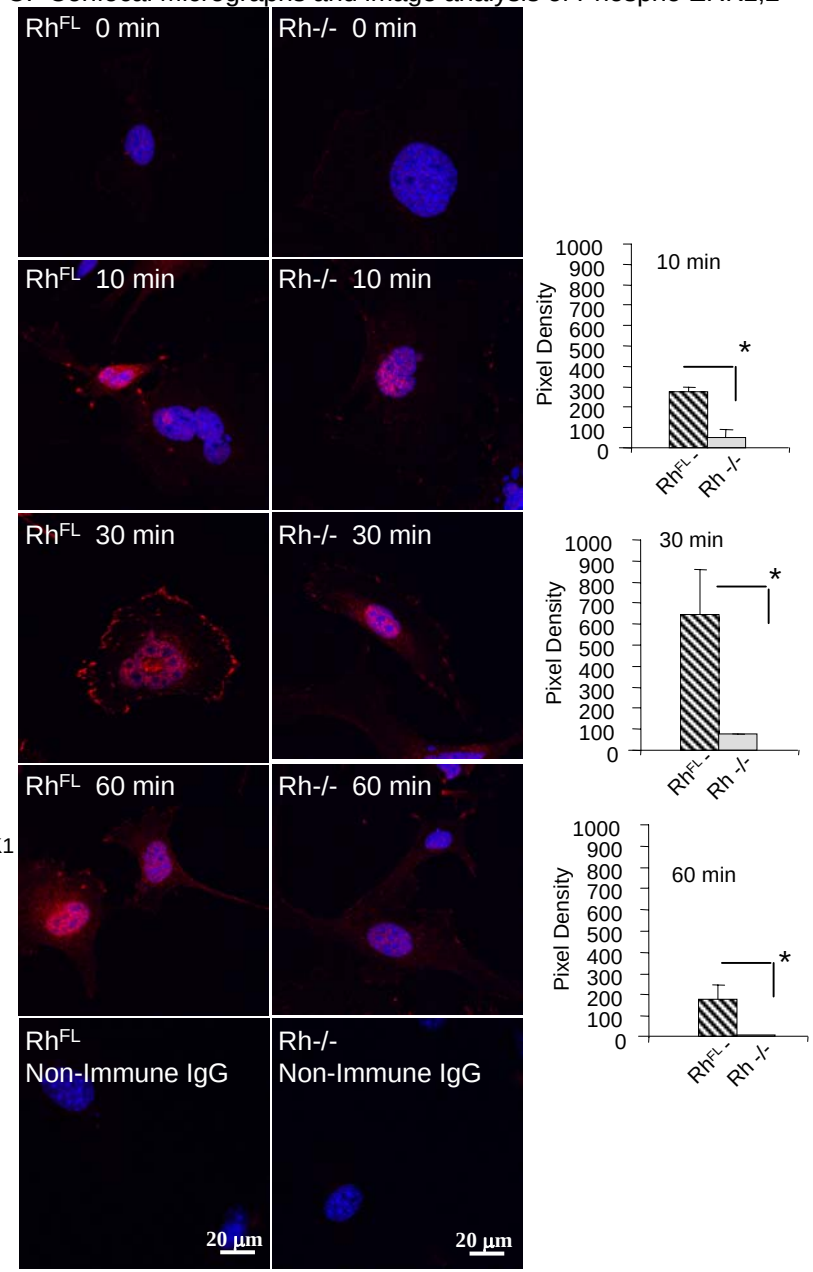

Figure 5. (Tolg et al.) Loss of Rhamm Reduces Migration and Invasion of Wt and Rh-/- Primary Fibroblasts

A. Migration Into Scratch Wounds in Response to FCS

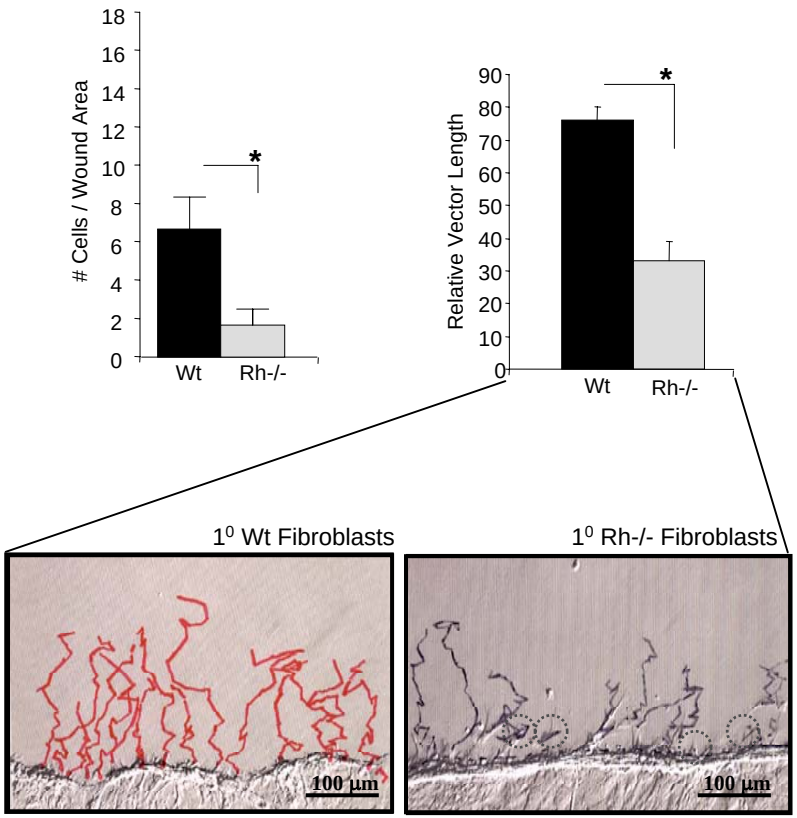

B. Invasion Into Collagen Gels in Response to PDGF

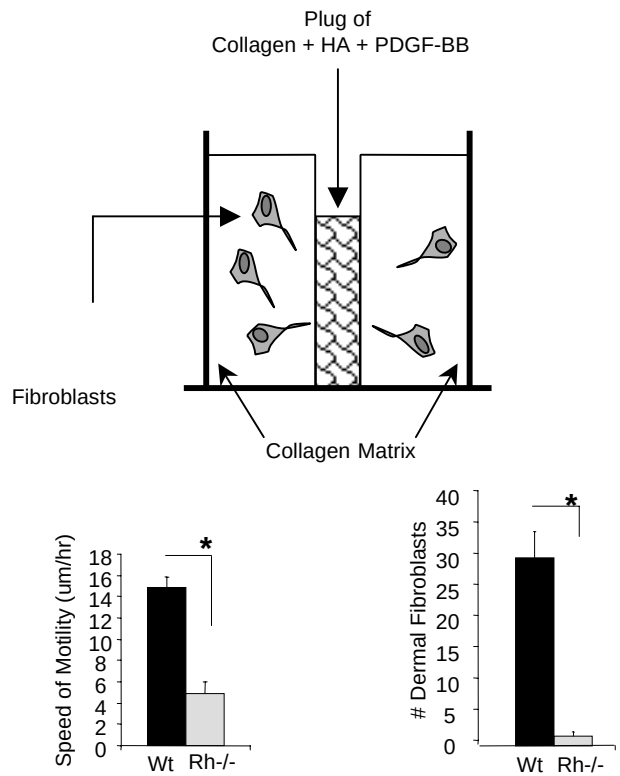

Figure 6. (Tolg et al.) CD44 Protein Co-Associates with Rhamm and Phospho-ERK1,2 in fibroblasts

A. CD44 Protein Expression

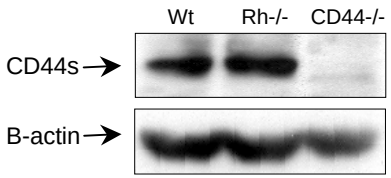

B. CD44 protein distribution

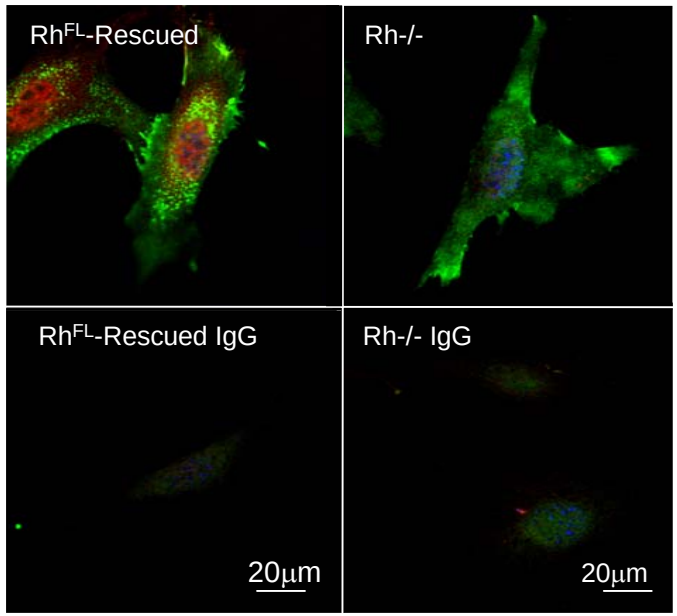

C. Rhamm, CD44 and ERK1,2 form Complexes

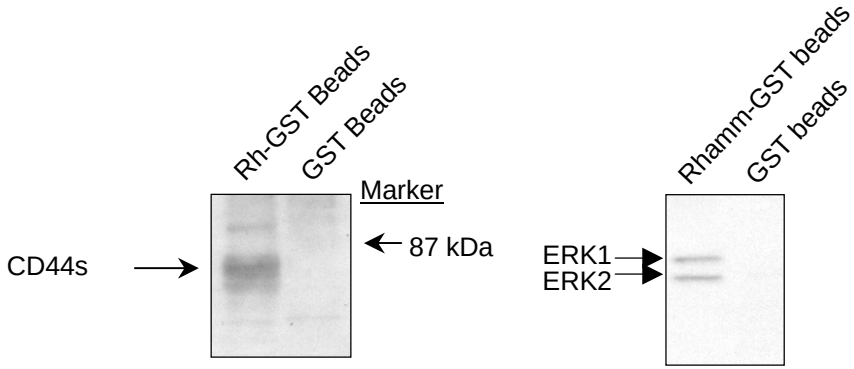

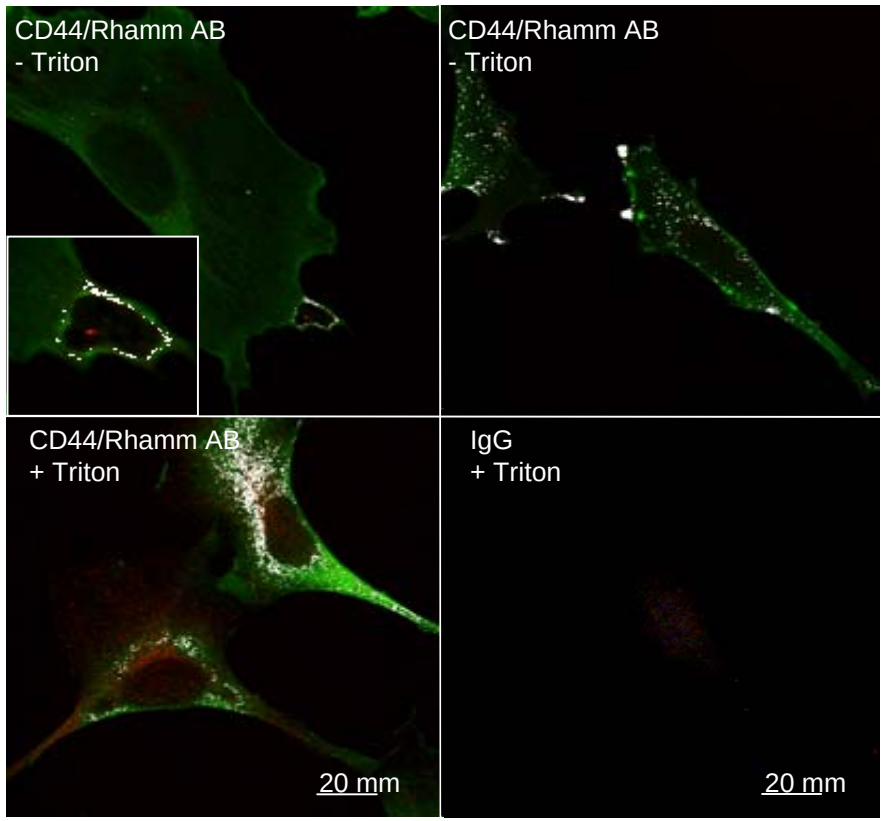

Figure 7. (Tolg et al.) Cell Surface Rhamm (CD168) and CD44 are Required for ERK1,2 Activity and for Motility in Response to FCS and HA

A. Role of CD168 (Rh) and CD44 in Nuclear ERK1,2 Activation

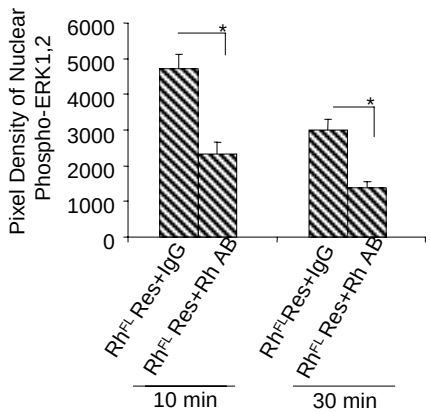

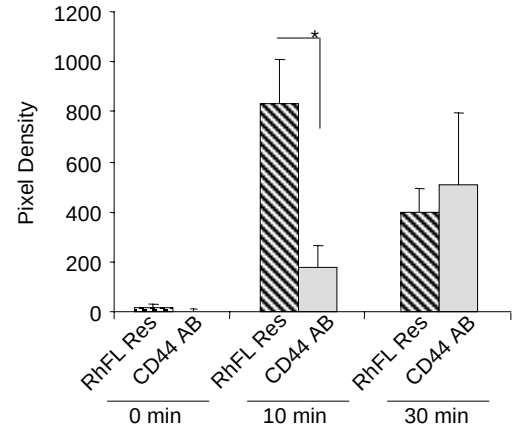

B. Rhamm^{FL}-Rescued Cell Motility in Response to FCS

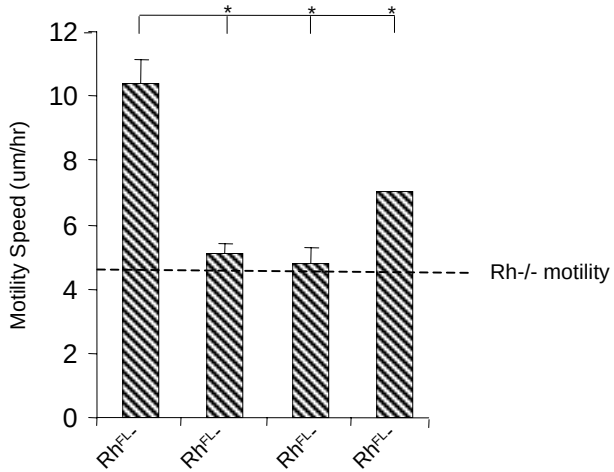

Rhamm Ab	-	+	-	-
Anti-CD44 Antibody	-	-	+	-
Non-Immune IgG	+	-	-	-
UO126	-	-	-	+

C. Rhamm^{FL}-Rescued Motility in Response to HA

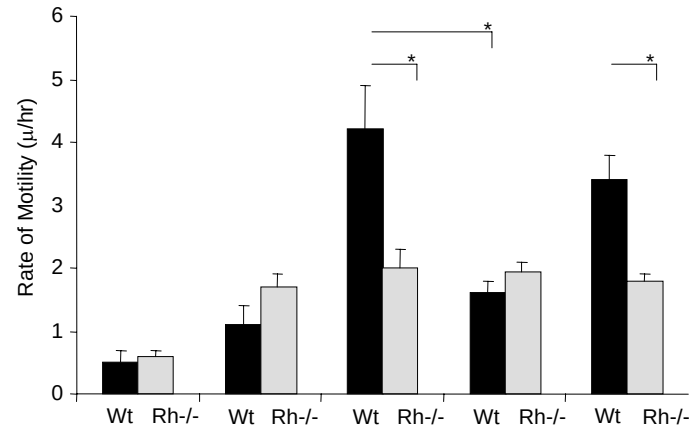

PMA	-	-	+	+	+	+	+	+	+	+
HA	-	-	-	-	+	+	+	+	+	+
Anti-Rh Antibody	-	-	-	-	-	-	+	+	-	-
IgG	-	-	-	-	-	-	-	-	+	+

Figure 8. (Tolg et al.) CD44 Cell Surface Display is ERK- and Cell Surface Rhamm- Dependant and Rhamm Promotes CD44/Phospho ERK 1, 2 Colocalization.

A. Effect of Rhamm on Cell Surface CD44 Expression

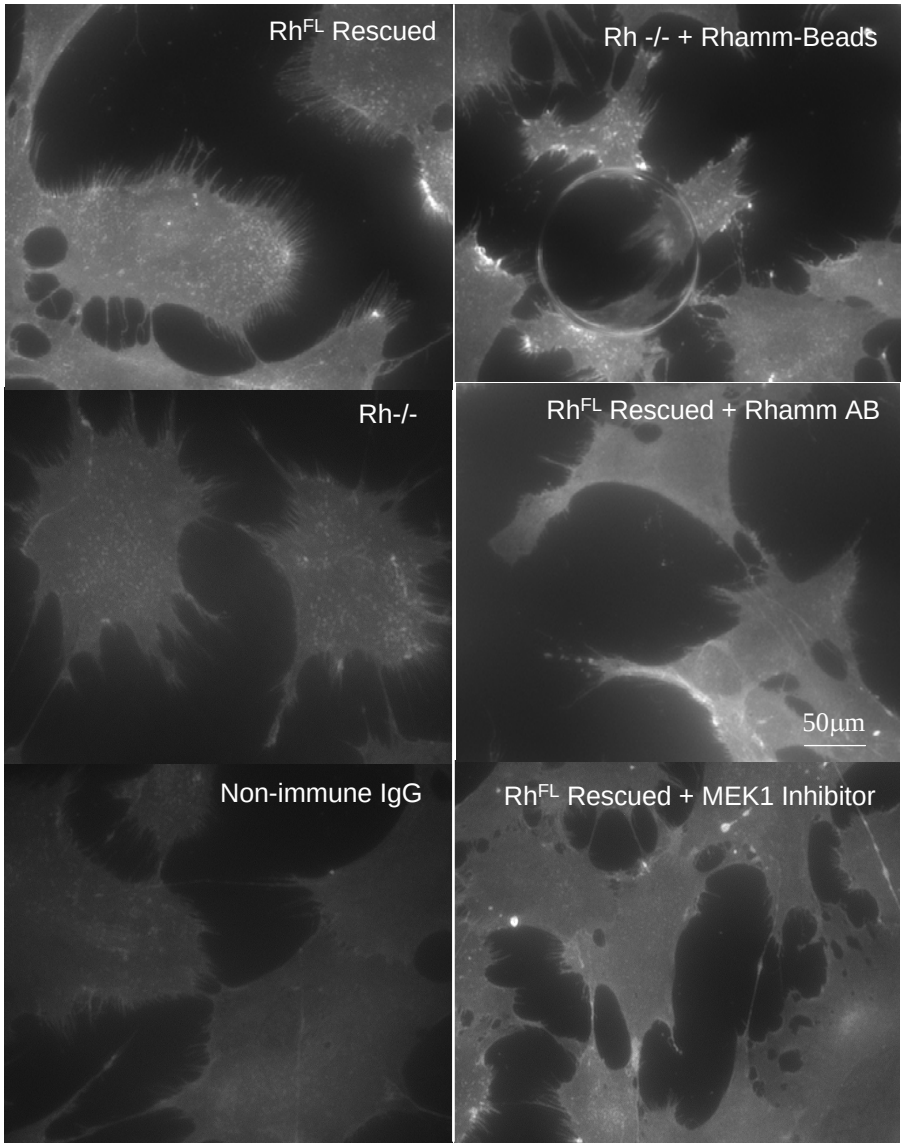

B. Effect of Rhamm on CD44 and Active ERK1,2 Co-Localization

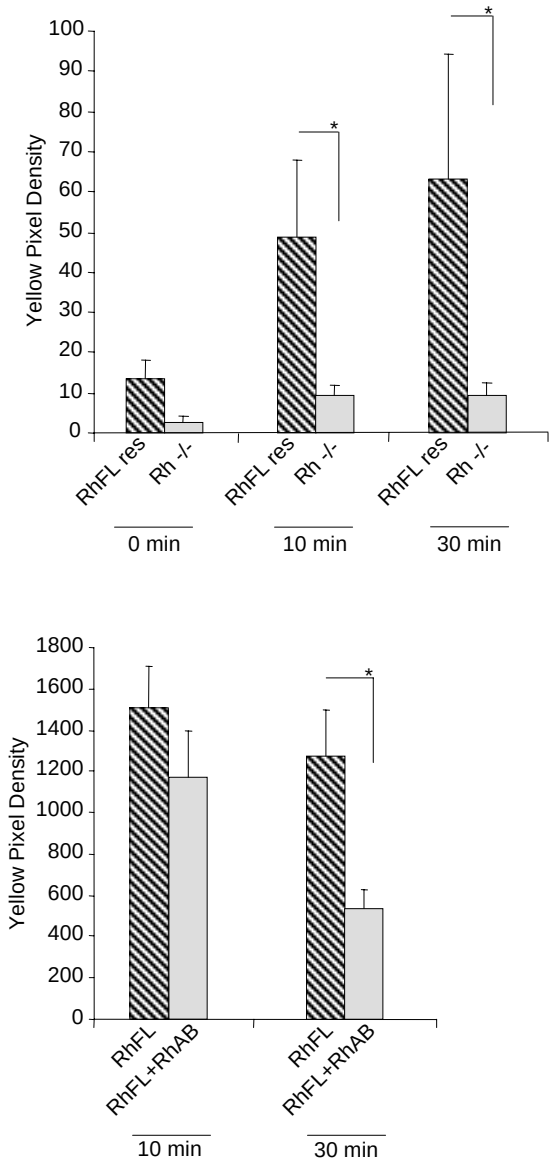

Figure 9. (Tolg et al.) Mutant Active Mek1 Rescues Aberrant ERK1,2 Activity, Motility and CD44 cell surface display in Rhamm-/- Fibroblasts

A. ELISA Analysis of ERK1,2 Activity

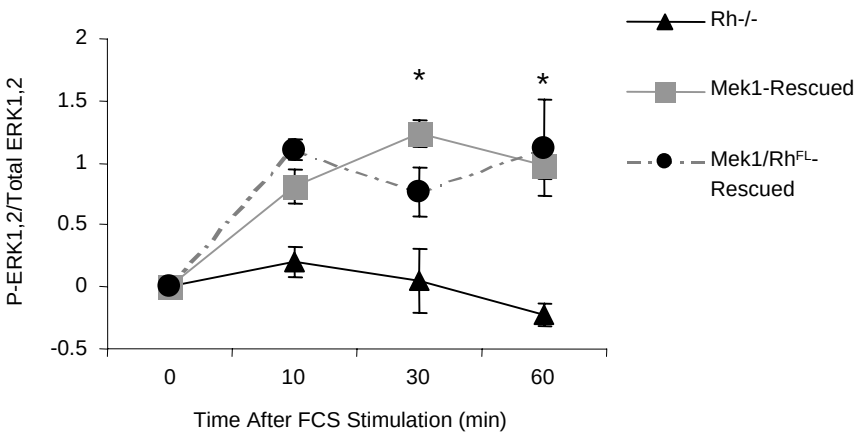

B. Western Blot Analysis of ERK1,2 Activity

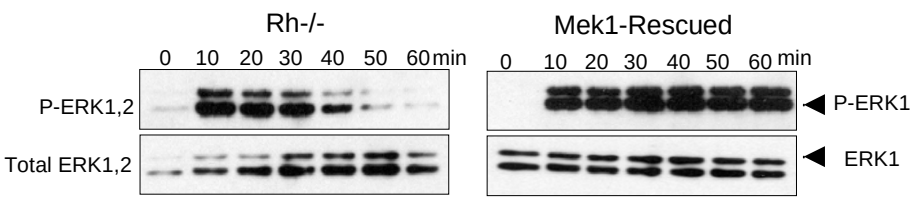

C. Motility and Cell Surface CD44 Display in Rh-/- Fibroblasts Expressing Mutant Active Mek1

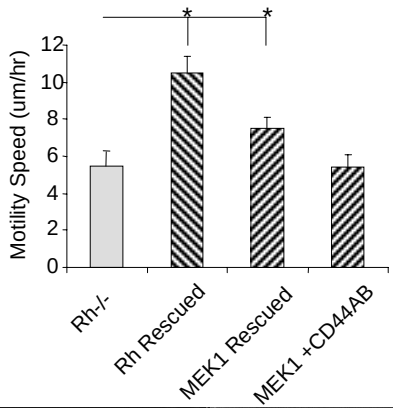

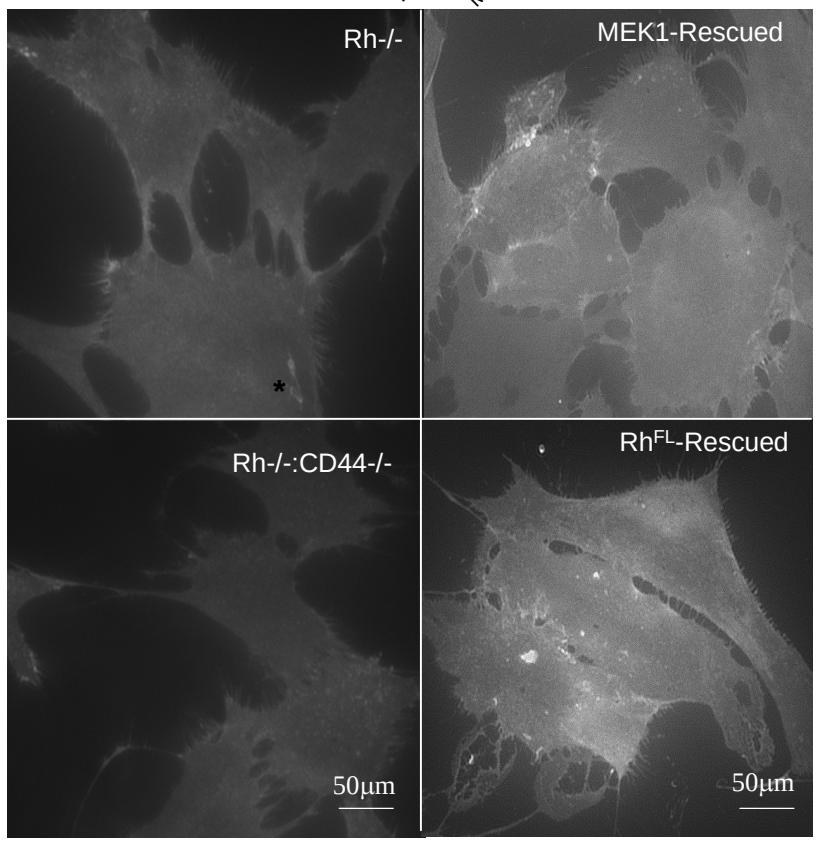

Figure 10. (Tolg et al.) Cell Surface Rhamm Rescues Motility Defect of Rhamm-/- Fibroblasts

A. Cell Motility in Response to Recombinant Rhamm Beads

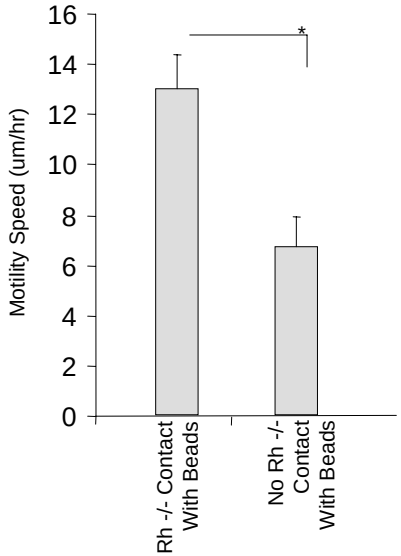

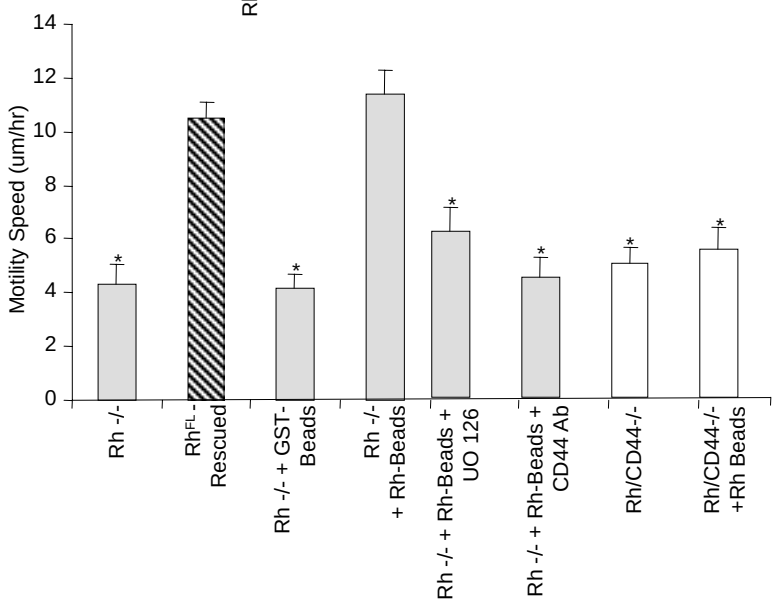

B. ERK1,2 Activation in Response to Recombinant Rhamm Beads

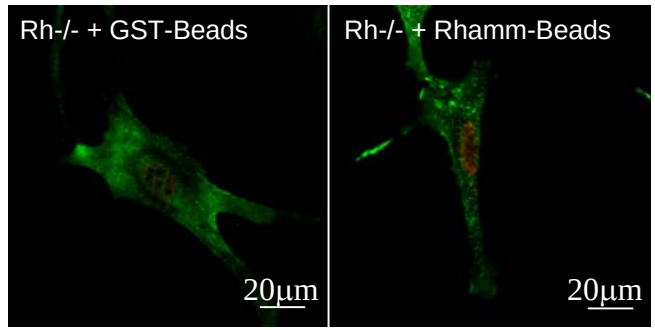

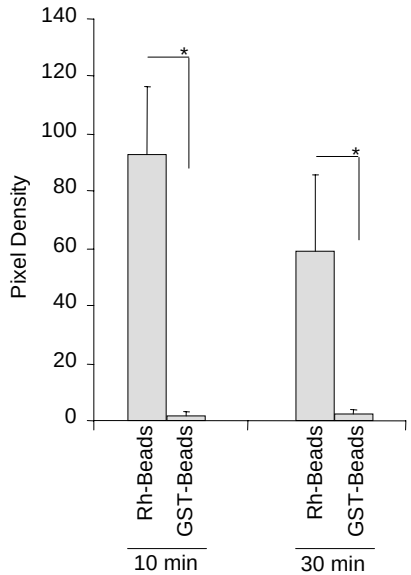

Supplemental Figure I. (Tolg et al.) Rhamm Expression is Regulated During Early Phases of Wound Repair and Loss of Rhamm Reduces Wound Contraction.

a. Rhamm Expression in Excisional Wounds

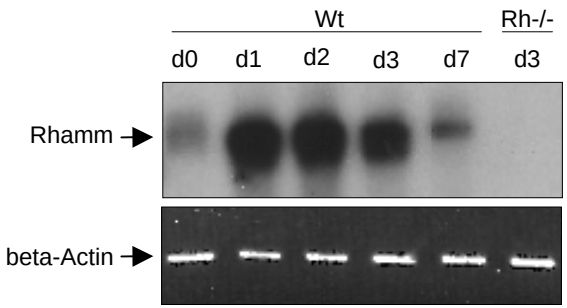

b. Macroscopic Quantification of Wound Contraction

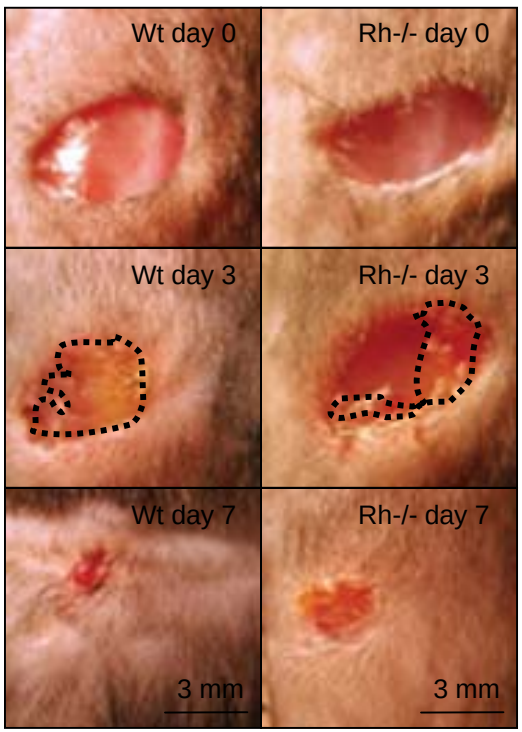

c. Microscopic Quantification of Wound Contraction

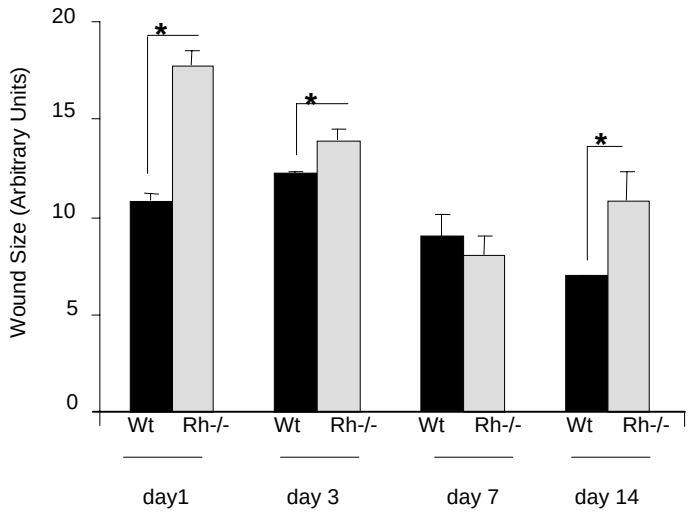

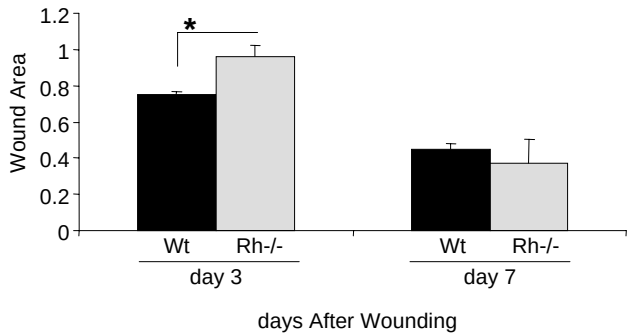

Supplemental Figure II. (Tolg et al.) Loss of Rhamm Expression Results in Aberrant Dermal Structure and Thickness in Both Uninjured and Repaired Skin

a. Dermis of Uninjured Skin

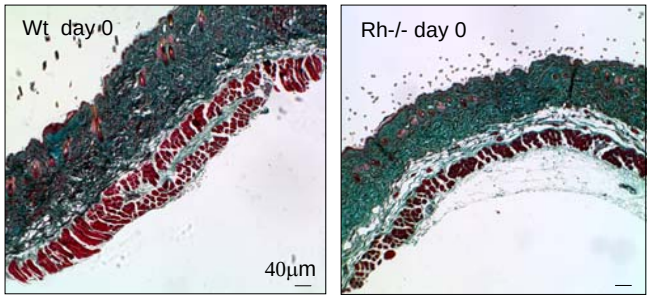

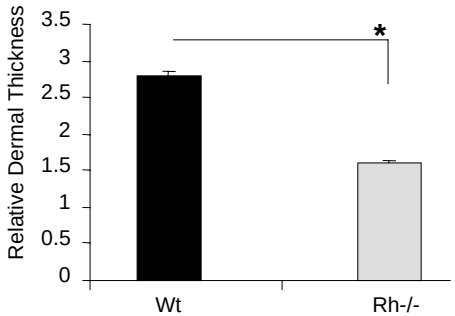
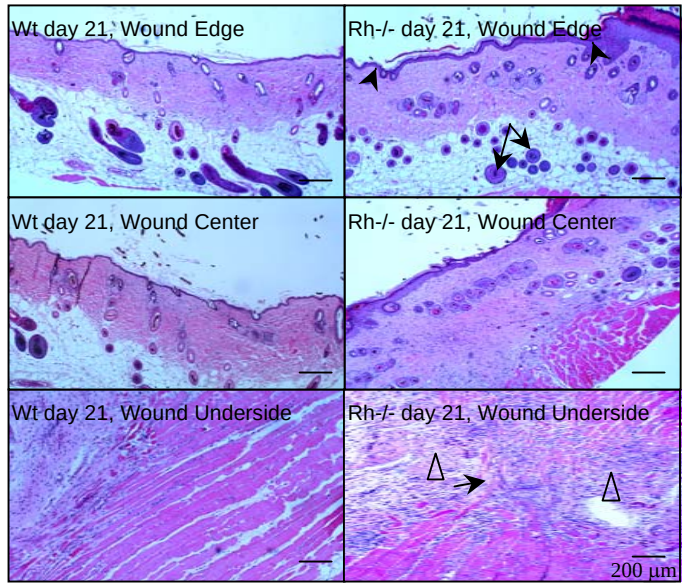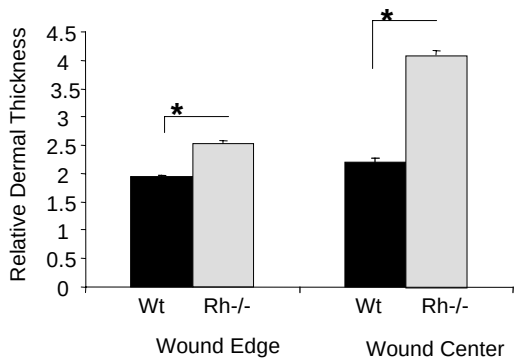
b. Dermis of Resolved Wounds